A PARTICLE DYNAMICS MODEL FOR THE SURFACE OPTIMIZATION OF A PELTON WHEEL BUCKET

By

RAKESH YADAV

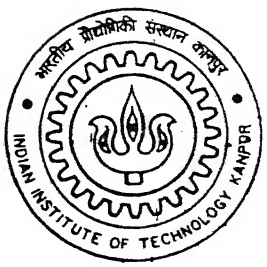

DEPARTMENT OF MECHANICAL ENGINEERING

Indian Institute of Technology Kanpur

JANUARY, 2002

A PARTICLE DYNAMICS MODEL FOR THE SURFACE OPTIMIZATION OF A PELTON WHEEL BUCKET

A Thesis Submitted

in Partial Fulfillment of the Requirements

for the Degree of

Master of Technology

by

RAKESH YADAV

DEPARTMENT OF MECHANICAL ENGINEERING

INDIAN INSTITUTE OF TECHNOLOGY KANPUR

Jan, 2002

CERTIFICATE

It is certified that the work contained in the thesis entitled, "A particle dynamics model for the surface optimization of a Pelton Wheel bucket" by Rakesh Yadav, has been carried out under my supervision and this work has not been submitted elsewhere for a degree.

3/1/02

Dr. V.Eswaran
Professor
Department of Mechanical Engg.
I. I. T. Kanpur

dedicated to

my grandmother

Acknowledgements

I would like to express my deep sense of gratitude and appreciation to my thesis supervisor Dr.V. Eswaran for the skillful guidance, constant supervision, timely suggestions in carrying out the present work.

I extend my profound thanks to all my friends, who made my stay memorable one. I am very grateful to my colleagues Atul Sharma, Arnab Kumar De and Abir Banerjee, for the encouragement I received from them. I am thankful to all members of HLX department of BHEL Bhopal for their timely suggestions and feedback.

I owe a lot to my wife for her loving support throughout the venture. This work could not been completed without the blessings of my parents. Even to think of thanking them is to trivialise all that they have done for me. My profoundest debts to them therefore, remain silent and unacknowledged.

Rakesh Yadav

IIT Kanpur

Jan, 2002

Contents

List of Figures

List of Tables

Abstract

The aim of the present work is to develop a computer program to compute the performance parameters like torque, power and efficiency of a Pelton Wheel with a given bucket surface configuration. The water jet striking the Pelton Wheel buckets is modeled as a series of particles. The force and the torque exerted by every particle, both on impact and subsequently during the motion on bucket, are computed, using Newtonian dynamics, at every instant of time and integrated over entire time span until they lose contact from the bucket. The time history of all particles is then used to obtain the total torque obtained by the water jet, as a function of time. The bucket shape is represented in local spherical coordinates $r = f(\theta, \phi)$ for which data are supplied on a coarse empirically measured xyz co-ordinate grid system. The performance parameters for two Pelton Wheel buckets are calculated with the present model and their results are compared. The aim is to help in the optimum design of Pelton Wheel buckets, both in terms of operating conditions and bucket surface profile

Chapter 1

Introduction

The purpose of a hydraulic turbine is to convert kinetic and potential energy of water into mechanical work. On the basis of the available head, three principal types of turbines - impulse turbine, the radial or mixed-flow reaction turbine, and the axial flow, or propeller, reaction turbine can be used.

Among the impulse water turbines, the Pelton turbine also called the free jet turbine, is the only type being mostly used these days. It is a high head and low flow turbine. The head of the supply water is converted into one or more high-velocity free jets which are directed against buckets mounted on the rim of a wheel. The impact of water on the surface of the bucket and further motion on the surface of the bucket produces a force which causes the wheel to rotate, thus supplying the mechanical power to the shaft.

In general, each bucket of Pelton Wheel consists of two nearly hemispherical cups separated by a sharp edge at the center. The water jet impinges at the center

of the bucket and is divided by the sharp edge, without shock, into two parts moving sideways in opposite directions. The water after impinging on the buckets is deflected through an angle of about 165° (instead of 180°), so that it may not strike the back of the other buckets and retard the motion of the wheel. The change in the momentum due to this change of directions transmits an 'impulse' torque to the bucket which translates to work output.

The efficiency of the wheel is given as

$$\eta = \frac{work\ done\ on\ the\ bucket}{energy\ supplied\ to\ the\ bucket}$$

The efficiency of the Pelton wheel is generally high (>90%). Therefore if improvement has to be made, we need to have analytical methods that can detect the effects of subtle changes in the bucket shape. Since the shape of the bucket plays a very important role in creating the torque, if the bucket surface is not proper the kinetic energy and momentum of the jet is not transferred efficiently to the bucket. An improper surface may cause too great a loss of kinetic energy as the jet impacts the bucket, and/or allow too much energy to leave with the water exiting the bucket. So the optimum surface and the optimum operating condition, a combination of which gives maximum efficiency, is required. In most text books, two dimensional analysis is presented using velocity triangles for the calculation of work done on the bucket. This simple analysis is not adequate since it does not consider the surface geometry, except the deflected angle. Through experiments we can also analyze the effect of the bucket surface on the power developed by

the wheel. But changing bucket parameters and doing experiment requires a lot of time as well as resources.

It would therefore, be of great help to the designer if a computational method can be found to theoretically evaluate the efficiency and other performance parameters of a proposed bucket shape. The speed and relatively low cost of computational solutions will allow the designer to evaluate many possible bucket shapes before actually constructing prototypes for experimental testing. This problem, though an important one, has virtually no published work. The commercial importance of the problem has ensured that any research on this problem is kept secret.

The general problem can be stated deceptively simply: Given a particular bucket shape, can its performance in terms of efficiency, torque, force and power generation be predicted? The problem is a very difficult one. Any attempt to obtain answers through the traditional routes of fluid mechanics seems to be currently impossible- for the jet/bucket interaction involves a highly unsteady, even turbulent, flow in a complex geometry involving free surfaces. To attempt to solve for flow using Euler or Navier Stokes equations seems to be completely outside the scope of present-day computational fluid dynamics.

In this thesis a method, far simpler and probably more likely to succeed, is attempted. The jet is treated as a steady stream of perfectly plastic (i.e, deformable) "particles" which strike the bucket and slide on its surface imparting momentum and energy to the bucket during their impact and subsequent motion on bucket surface. The particles are assumed to be non-interacting (i.e the motion of each such

"particle" is taken to be independent of others) and the motion of each particle is computed using the Newtonian laws governing particle motion. The equations governing the particle motion are coupled second-order ordinary differential equations (much more numerically tractable than the partial differential equations of fluid flow) which can be solved by the Runge-Kutta method. However, considerable difficulty is introduced into the problem due to the generally complex bucket geometry involved. Once the time history of each particle is known from the solution of the dynamical equations, the effects of all particles can be integrated to obtain the total picture regarding the efficiency, torque etc., generated by the bucket.

In the present work, we have followed the work of Ajay Kumar (1999) to develop a set of computer programs to analyze the performance of real-life working Pelton Wheel buckets. If the number of buckets in the proposed design are not fixed then the simulations are done for single bucket, but the program can simulate more than one bucket sharing the jet at a time. The torque imparted to the bucket is computed at every instant of time and integrated over the entire time span. The geometry of the bucket is usually very complex and is very important in the calculation of torque. Therefore the surface of the bucket is represented by a fine grid in spherical coordinates (r, θ, ϕ) having uniform intervals of θ and ϕ, with the value of r is specified at every grid point. Bi-linear interpolation is used to find the interpolated value at any intermediate point. We can change the parameters of the bucket and see the effects on the torque developed and study of the other parameters to tell which part (configuration of system or the bucket

surface profile or both) is to be improved/optimized. One test case of 3 D planner bucket is simulated with this program for the validation of the code.

This work was partly supported by a project sponsored by BHEL Bhopal. Performance parameters for two Real life working buckets with surface profiles and operating conditions are provided by BHEL Bhopal are also calculated. The effect of changing the various input parameters on the performance of the Pelton Wheel is studied with the program. The program basically has two parts, one for grid generation, which represents the surface of the bucket in the required coordinate system from empirically measured data, and other solves the governing equation over the grid representing the bucket surface to obtain the performance parameters.

This work is the culmination of the work which was started by Ajay Kumar (1999) and Gaurav Dar (2000). However, only here have all the necessary elements of the formulations developed by these previous authors been put together to compute the efficiencies etc. of real-life Pelton Wheel buckets provided by BHEL Bhopal.

Chapter 2

Theoretical Formulation

2.1 Introduction

As already discussed, because of inherent difficulties in the fluid mechanics approach to the detailed analyses of flow in a Pelton Wheel buckets, a particle dynamics approach is adopted here. In this the water jet striking the Pelton Wheel bucket is modeled as a series of particles. The momentum and energy transfer from these particles to the bucket is then computed by using the principles of momentum conservation and of Newton's second law applied to the individual particles. In this chapter, the kinematics and dynamics of the fluid particle in three dimensional (3D) situations is formulated. First we consider a 3D model for calculating the force and torque imparted on the rotating bucket by a single particle. A general shape of the bucket whose equation is given in polar coordinates is considered. Later, this model is extended for a series of continuous particles and

the concept of mass flow rate is introduced.

2.2 Kinematics and dynamics of a single particle for 3-dimensional bucket

Following Ajay Kumar (1999), let us consider a bucket of general shape rotating with a constant angular velocity ω about the X-axis as shown in figure 2.1(a). There are two frames of reference considered, one fixed frame XYZ centered at O, while other one moving frame xyz centered at o'. The frame xyz is attached to an extended point (o') of the arm whose distance from the origin of the fixed frame (i.e from O) is R. In figure 2.1(b), the bucket is represented in spherical coordinates which are fixed to the origin o' of the xyz coordinate system. The surface equation of the bucket is assumed to be $\psi(r, \theta, \phi) = 0$ and its gradient is given by

$$\nabla\vec{\psi} = \frac{\partial\psi}{\partial r}\hat{r} + \frac{1}{r}\frac{\partial\psi}{\partial\theta}\hat{\theta} + \frac{1}{r\sin\theta}\frac{\partial\psi}{\partial\phi}\hat{\phi} \tag{2.1}$$

Initially at $t = 0$, the arm is assumed to make an angle χ_0 from the Z-axis, a particle p_b traveling along the water jet parallel to the Y axis strikes the bucket at point p_{b0} with velocity $\vec{v}_j$. The position vector of p_{b0} with respect to the moving (r, θ, ϕ) frame is $r\hat{r} + \theta\hat{\theta} + \phi\hat{\phi}$. After striking the bucket at point p_{b0}, the particle is assumed to travel along the bucket. At that instant, absolute acceleration of the particle is along $-\nabla$, which is normal to the bucket surface (i.e. the bucket

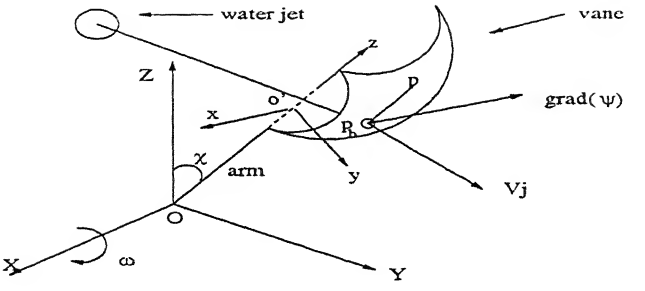

(a)

p =particle

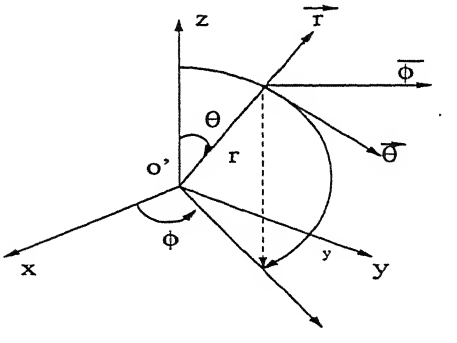

(b) Bucket in spherical co–ordinates

Figure 2.1: Schematic diagram of bucket in 3D

is assumed to be frictionless so the particle is subjected only to a normal force and experiences a normal acceleration). According to the laws of dynamics, the absolute acceleration of the particle p_b is given by

$$\vec{a}_{abs} = \vec{a}_0 + \vec{\omega} \times (\vec{\omega} \times \vec{r}) + 2\vec{\omega} \times (\dot{r}\vec{r} + r\dot{\theta}\hat{\theta} + r\sin\theta\dot{\phi}\hat{\phi}) + a_r\hat{r} + a_\theta\hat{\theta} + a_\phi\hat{\phi} \quad (2.2)$$

where $\vec{a}_0$ is the acceleration of point o'

$\vec{a}_0 = -\omega^2 R\hat{k}$

and a_r, a_θ, a_ϕ are the acceleration components of the point p_{b0} in $\hat{r}$, $\hat{\theta}$, $\hat{\phi}$ directions, respectively. These components are given as

$a_r = \ddot{r} - r\dot{\theta}^2 - r\dot{\phi}^2\sin^2\theta$

$a_\theta = r\ddot{\theta} + 2\dot{r}\dot{\theta} - r\dot{\phi}^2\sin\theta\cos\theta$

$a_\phi = r\ddot{\phi}\sin\theta + 2\dot{r}\dot{\phi}\sin\theta + 2r\dot{\theta}\dot{\phi}\cos\theta$

The relation between the unit vectors in the Cartesian coordinates and spherical coordinates for the moving frame are given as follows

$\hat{r} = \sin\theta\cos\phi\hat{i} + \sin\theta\sin\phi\hat{j} + \cos\hat{k}$

$\hat{\theta} = \cos\theta\cos\phi\hat{i} + \cos\theta\sin\phi\hat{j} - \sin\theta\hat{k}$

$\hat{\phi} = -\sin\phi\hat{i} + \cos\phi\hat{j}$

The above relations can also be written as

$$\begin{Bmatrix} \hat{i} \\ \hat{j} \\ \hat{k} \end{Bmatrix} = \begin{bmatrix} \sin\theta\cos\phi & \cos\theta\cos\phi & -\sin\phi \\ \sin\theta\sin\phi & \cos\theta\sin\phi & \cos\phi \\ \cos\theta & -\sin\theta & 0 \end{bmatrix} \begin{Bmatrix} \hat{r} \\ \hat{\theta} \\ \hat{\phi} \end{Bmatrix} \tag{2.3}$$

Also the relations between the Cartesian coordinates of the fixed frame and the moving frame are as follows;

$\hat{I} = \hat{i}$

$\hat{J} = \cos\chi\hat{j} + \sin\chi\hat{k}$

$\hat{K} = -\sin\chi\hat{j} + \cos\chi\hat{k}$

equation (2.2) can be written as

$$\vec{a}_{abs} = A_r\hat{r} + A_\theta\hat{\theta} + A_\phi\hat{\phi} \tag{2.4}$$

where

$$\begin{aligned} A_r &= -\omega^2 R\cos\theta - \omega^2 r(\cos^2\theta\cos^2\phi + \sin^2\phi) - 2\omega r(\dot{\phi}\cos\theta\sin\theta \\ &\quad \cos\phi + \dot{\theta}\sin\phi) + (\ddot{r} - r\dot{\theta}^2 - r\dot{\phi}^2\sin^2\theta), \end{aligned} \tag{2.5}$$

$$\begin{aligned} A_\theta &= \omega^2 R\sin\theta + \omega^2 r\sin\theta\cos\theta\cos^2\phi + \dot{\omega}r\sin\phi + 2\omega(r\dot{\phi}\sin^2\theta \\ &\quad + \dot{r}\sin\phi) + (r\ddot{\theta} + 2\dot{r}\dot{\theta} - r\dot{\phi}^2\sin\theta\cos\theta), \end{aligned} \tag{2.6}$$

and

$$A_\phi = -\omega^2 r\sin\theta\cos\phi\sin\phi + \dot{\omega}r\cos\theta\cos\phi + 2\omega(\dot{r}\cos\theta\cos\phi - \\ -r\dot{\theta}\sin\theta\cos\phi) + (r\ddot{\phi}\sin\theta + \dot{2}\dot{r}\dot{\phi}\sin\theta + 2r\dot{\theta}\dot{\phi}\cos\theta). \quad (2.7)$$

However, as the bucket is assumed frictionless, the net force on the particle, and hence its absolute acceleration, can only normal to the bucket surface, i.e., in the direction of $-\nabla\psi$.This implies a relationship between the magnitudes of A_r, A_θ, A_ϕ such that the resultant acceleration is in the normal direction, following two equations are thus obtained.

$$\frac{A_r}{\frac{\partial\psi}{\partial r}} = \frac{A_\theta}{\frac{1}{r}\frac{\partial\psi}{\partial\theta}} \quad (2.8)$$

and

$$\frac{A_r}{\frac{\partial\psi}{\partial r}} = \frac{A_\phi}{\frac{1}{r\sin\theta}\frac{\partial\psi}{\partial\phi}} \quad (2.9)$$

along with

$$\psi(r,\theta,\phi) = 0 \quad (2.10)$$

Substituting equation 2.10 in equations 2.8 and 2.9 and using expressions (2.5, 2.6 and 2.7) we get

$$a_{11}\ddot{\theta} + a_{12}\ddot{\phi} + a_{13}\dot{\theta}^2 + a_{14}\dot{\phi}^2 + a_{15}\dot{\phi} + a_{16}\dot{\theta}\dot{\phi} + c = 0 \qquad (2.11)$$

and

$$a_{21}\ddot{\theta} + a_{22}\ddot{\phi} + a_{23}\dot{\theta}^2 + a_{24}\dot{\phi}^2 + a_{25}\dot{\theta} + a_{26}\dot{\theta}\dot{\phi} + d = 0 \qquad (2.12)$$

where all a's are function of geometric variables and are as follows

$$a_{11} = (-\frac{1}{r}\frac{(\frac{\partial\psi}{\partial\theta})^2}{\frac{\partial\psi}{\partial r}} - r\frac{\partial\psi}{\partial r})$$

$$a_{12} = -\frac{1}{r}\frac{\frac{\partial\psi}{\partial\theta}\frac{\partial\psi}{\partial\phi}}{\frac{\partial\psi}{\partial r}}$$

$$a_{13} = \frac{2}{r}\frac{(\frac{\partial\psi}{\partial\theta})^2\frac{\partial^2\psi}{\partial r\partial\theta}}{(\frac{\partial\psi}{\partial r})^2} - \frac{1}{r}\frac{\frac{\partial^2\psi}{\partial r^2}(\frac{\partial\psi}{\partial\theta})^3}{(\frac{\partial\psi}{\partial r})^3} - \frac{1}{r}\frac{\frac{\partial^2\psi}{\partial\theta^2}\frac{\partial\psi}{\partial\theta}}{\frac{\partial\psi}{\partial r}} + \frac{\partial\psi}{\partial\theta}$$

$$a_{14} = 2\frac{1}{r}\frac{\frac{\partial^2\psi}{\partial r\partial\phi}\frac{\partial\psi}{\partial\theta}\frac{\partial\psi}{\partial\phi}}{(\frac{\partial\psi}{\partial r})^2} - \frac{1}{r}\frac{\frac{\partial^2\psi}{\partial r^2}\frac{\partial\psi}{\partial\theta}(\frac{\partial\psi}{\partial\phi})^2}{(\frac{\partial\psi}{\partial r})^3} - \frac{1}{r}\frac{\frac{\partial^2\psi}{\partial\phi^2}\frac{\partial\psi}{\partial\theta}}{\frac{\partial\psi}{\partial r}} - \sin^2\theta\frac{\partial\psi}{\partial\theta}$$
$$+r\sin\theta\cos\theta\frac{\partial\psi}{\partial r}$$

$$a_{15} = -2\omega\cos\theta\sin\theta\cos\phi\frac{\partial\psi}{\partial\theta} - 2\omega r\sin^2\theta\cos\phi\frac{\partial\psi}{\partial r} + 2\omega\sin\phi\frac{\partial\psi}{\partial\phi}$$

$$a_{16} = \frac{2}{r}\frac{\frac{\partial^2\psi}{\partial r\partial\theta}\frac{\partial\psi}{\partial\theta}\frac{\partial\psi}{\partial\phi}}{(\frac{\partial\psi}{\partial r})^2} + \frac{2}{r}\frac{\frac{\partial^2\psi}{\partial r\partial\phi}(\frac{\partial\psi}{\partial\theta})^2}{(\frac{\partial\psi}{\partial r})^2} - \frac{2}{r}\frac{\frac{\partial^2\psi}{\partial\theta\partial\phi}\frac{\partial\psi}{\partial\theta}}{\frac{\partial\psi}{\partial r}} - \frac{2}{r}\frac{\frac{\partial^2\psi}{\partial r^2}(\frac{\partial\psi}{\partial\theta})^2\frac{\partial\psi}{\partial\phi}}{(\frac{\partial\psi}{\partial r})^3}$$
$$+2\frac{\partial\psi}{\partial\phi}$$

$$c = -\frac{1}{r}\frac{\partial\psi}{\partial\theta}(\omega^2 R\cos\theta + \omega^2 r(\cos^2\theta\cos^2\phi + \sin^2\phi)) - \frac{\partial\psi}{\partial r}(\omega^2 R\sin\theta$$

$$+\omega^2 r \sin\theta \cos\theta \cos^2\phi + \dot{\omega} r \sin\phi)$$

$$a_{21} = -\frac{1}{r\sin\theta}\frac{\frac{\partial\psi}{\partial\theta}\frac{\partial\psi}{\partial\phi}}{\frac{\partial\psi}{\partial r}}$$

$$a_{22} = -\frac{1}{r\sin\theta}\frac{(\frac{\partial\psi}{\partial\phi})^2}{\frac{\partial\psi}{\partial r}} - r\sin\theta\frac{\partial\psi}{\partial r}$$

$$a_{23} = \frac{2}{r\sin\theta}\frac{\frac{\partial^2\psi}{\partial r\partial\theta}\frac{\partial\psi}{\partial\theta}\frac{\partial\psi}{\partial\phi}}{(\frac{\partial\psi}{\partial r})^2} - \frac{1}{r\sin\theta}\frac{\frac{\partial^2\psi}{\partial r^2}(\frac{\partial\psi}{\partial\theta})^2\frac{\partial\psi}{\partial\phi}}{(\frac{\partial\psi}{\partial r})^3} - \frac{1}{r\sin\theta}\frac{\frac{\partial^2\psi}{\partial\theta^2}\frac{\partial\psi}{\partial\phi}}{\frac{\partial\psi}{\partial r}} - \frac{1}{\sin\theta}\frac{\partial\psi}{\partial\phi}$$

$$a_{24} = \frac{2}{r\sin\theta}\frac{\frac{\partial^2\psi}{\partial r\partial\phi}(\frac{\partial\psi}{\partial\phi})^2}{(\frac{\partial\psi}{\partial r})^2} - \frac{1}{r\sin\theta}\frac{\frac{\partial^2\psi}{\partial r^2}(\frac{\partial\psi}{\partial\phi})^3}{(\frac{\partial\psi}{\partial r})^3} - \frac{1}{r\sin\theta}\frac{\frac{\partial^2\psi}{\partial\phi^2}\frac{\partial\psi}{\partial\phi}}{\frac{\partial\psi}{\partial r}} + \sin\theta\frac{\partial\psi}{\partial\phi}$$

$$a_{25} = -\frac{2\omega\sin\phi}{\sin\theta}\frac{\partial\psi}{\partial\phi} + 2\omega\cos\theta\cos\phi\frac{\partial\psi}{\partial\theta} + 2\omega r\sin\theta\cos\phi\frac{\partial\psi}{\partial r}$$

$$a_{26} = \frac{2}{r\sin\theta}\frac{\frac{\partial^2\psi}{\partial r\partial\theta}(\frac{\partial\psi}{\partial\phi})^2}{(\frac{\partial\psi}{\partial r})^2} + \frac{2}{r\sin\theta}\frac{\frac{\partial^2\psi}{\partial r\partial\phi}\frac{\partial\psi}{\partial\theta}\frac{\partial\psi}{\partial\phi}}{(\frac{\partial\psi}{\partial r})^2} - \frac{2}{r\sin\theta}\frac{\frac{\partial^2\psi}{\partial\theta\partial\phi}\frac{\partial\psi}{\partial\phi}}{\frac{\partial\psi}{\partial r}} - \frac{2}{r\sin\theta}$$
$$\frac{\frac{\partial^2\psi}{\partial r}\frac{\partial\psi}{\partial\theta}(\frac{\partial\psi}{\partial\phi})^2}{(\frac{\partial\psi}{\partial r})^3} - 2r\cos\theta\frac{\partial\psi}{\partial r} + 2\sin\theta\frac{\partial\psi}{\partial\theta}$$

$$d = \frac{1}{r\sin\theta}\frac{\partial\psi}{\partial\phi}(-\omega^2 R\cos\theta - \omega^2 r(\cos^2\theta\cos^2\phi + \sin^2\phi)) - \frac{\partial\psi}{\partial r}(-\omega^2 r$$
$$\sin\theta\cos\phi\sin\phi + \dot{\omega} r\cos\theta\cos\phi)$$

Equations (2.11 and 2.12) governing the motion of the particle on the bucket surface, are two coupled second order non-linear ordinary differential equations in θ and ϕ. These can be solved simultaneously as initial value problem, and will require four initial conditions in terms of θ_0, ϕ_0, $\dot{\theta}_0$ and $\dot{\phi}_0$ (i.e. the values of θ, $\dot{\theta}$, ϕ and $\dot{\phi}$ at $t = 0$). The value of θ_0 and ϕ_0 can be calculated by determining

the point at which the particle path along the water jet meets the bucket surface. The methodology to obtain θ_0 and ϕ_0 will be discussed in detail later on. Once the particle's initial position (θ_0,ϕ_0) has been obtained, then to find the values of $\dot{\theta}$ and $\dot{\phi}$ at $t = 0$, we proceed as follows:

As discussed in the previous section, after the initial impact the component of jet velocity $\vec{v}_j$ along $\nabla\vec{\psi}$ is same as the velocity of the point p_{b0} on the bucket surface in that direction but the velocity of the jet is unchanged in the direction normal to $\nabla\vec{\psi}$, i.e. tangential to the surface. This is because no force could be applied tangential to the surface of the buckets (which is frictionless), thus the tangential momentum of the particle will remain unchanged.

Before impact, the velocity of the jet tangential to the surface is

$$\mathbf{v}_j - \frac{(\mathbf{v}_j.\nabla\psi)\nabla\psi}{|\nabla\psi|^2} \tag{2.13}$$

and the tangential velocity of the particle after impact is

$$\mathbf{v}_p - \frac{(\mathbf{v}_p.\nabla\psi)\nabla\psi}{|\nabla\psi|^2} \tag{2.14}$$

where $\mathbf{v}_p$ is the total velocity of the particle after impact,

As the tangential velocity of the particle remains unchanged after impact,

$$\mathbf{v}_j - \frac{(\mathbf{v}_j.\nabla\psi)\nabla\psi}{|\nabla\psi|^2} = \mathbf{v}_p - \frac{(\mathbf{v}_p.\nabla\psi)\nabla\psi}{|\nabla\psi|^2} \tag{2.15}$$

and the normal velocity of the particle after impact is equal to the velocity of the

bucket at the point of impact, i.e.,

$$\mathbf{v}_p.\nabla\psi = \mathbf{v}_{pb}.\nabla\psi \tag{2.16}$$

where $\mathbf{v}_{pb} = \omega \times (R\hat{k} + r\hat{r})$ is the velocity of the bucket surface at the point of impact. We can also express $\mathbf{v}_p$ as :

$$\mathbf{v}_p = \omega \times (R\hat{k} + r\hat{r}) + \dot{r}\hat{r} + r\dot{\theta}\hat{\theta} + rsin\theta\dot{\phi}\hat{\phi} \tag{2.17}$$

where the first expression on the right is v_{pb} and the remaining terms are the relative velocities (wrt point pb) in the r, θ, ϕ directions. Substituting the above expression for v_p into equation (2.15) and using equation (2.16) we get

$$\mathbf{v}_j - \frac{(\mathbf{v}_j.\nabla\psi)\nabla\psi}{|\nabla\psi|^2} + \frac{(\mathbf{v}_{pb}.\nabla\psi)\nabla\psi}{|\nabla\psi|^2} = \omega \times (R\hat{k} + r\hat{r}) + \dot{r}\hat{r} + r\dot{\theta}\hat{\theta} + rsin\theta\dot{\phi}\hat{\phi} \tag{2.18}$$

Now

$$\mathbf{v}_j = v_j cos\chi\hat{j} + v_j sin\chi\hat{k} \tag{2.19}$$

Replacing the unit vectors $\hat{i}, \hat{j}, \hat{k}$ by $\hat{r}, \hat{\theta}, \hat{\phi}$ in equation (2.19) by using (2.3), and then substituting into equation (2.18) and equating the two sides component-wise we get,

$$\dot{\theta}_0 = \frac{-\omega R cos\theta sin\phi - \frac{\mathbf{v}_j.\nabla\psi}{|\nabla\psi|^2}\frac{1}{r}\frac{\partial\psi}{\partial\theta} + \frac{\mathbf{v}_{pb}.\nabla\psi}{|\nabla\psi|^2}\frac{1}{r}\frac{\partial\psi}{\partial\theta} + \mathbf{v}_j(cos\chi cos\theta sin\phi - sin\chi sin\theta) - \omega r sin\phi}{r} \tag{2.20}$$

and

$$\dot{\phi}_0 = \frac{-\omega R cos\phi - \frac{\mathbf{v}_j.\nabla\psi}{|\nabla\psi|^2}\frac{1}{r}\frac{\partial\psi}{\partial\theta} + \frac{\mathbf{v}_{pb}.\nabla\psi}{|\nabla\psi|^2}\frac{1}{r}\frac{\partial\psi}{\partial\theta} + \mathbf{v}_j cos\chi cos\phi - \omega r cos\theta cos\phi}{r sin\theta} \tag{2.21}$$

In this manner we arrive at two of the four initial conditions required for the particle path computation.

2.3 Particle Force and torque computation

Equations (2.11) and (2.12) which govern the motion of each particle on the bucket surface are two coupled second-order non-linear ordinary differential equations, and are solved as initial value problem which require four initial condition in terms of θ, $\dot{\theta}$, ϕ, $\dot{\phi}$. All the four quantities (θ, $\dot{\theta}$, ϕ, $\dot{\phi}$) at the subsequent time steps (starting from the impact time t_{pi} to the time the particle leaves the bucket) are calculated by solving the equations (2.11and 2.12) using a fourth order Runge-Kutta (RK4) solution method. the change in θ, $\dot{\theta}$, ϕ, $\dot{\phi}$ with time is used to calculate the velocity and the acceleration at every time step. The particle is considered to have left the bucket whenever the computed a_n (normal acceleration) becomes

negative or the particle reaches the edge of the bucket. Using these values, we get $\vec{a}_{abs}$ (absolute acceleration) from the equation (2.4). The force exerted by the single particle is given by

$$\mathbf{F} = -m_p a_{abs} \tag{2.22}$$

where, m_p ($= \dot{m}_p \Delta t$) is the mass of the particle, $\dot{m}_p$ is the mass flow rate.

The initial impulse exerted by the particle during the first impact at p_{b0} is obtained as

$$\mathbf{I}_n = m_p\left(\frac{\vec{v}_j.\nabla\psi}{|\nabla\psi|} - \frac{\vec{v}_{pb}.\nabla\psi}{|\nabla\psi|}\right) \tag{2.23}$$

and the average force is taken to be

$$\mathbf{F}_n = \dot{m}_p\left(\frac{\vec{v}_j.\nabla\psi}{|\nabla\psi|} - \frac{\vec{v}_{pb}.\nabla\psi}{|\nabla\psi|}\right) \tag{2.24}$$

where $\vec{v}_{pb} = \omega \times (R\hat{k} + r\hat{r})$

Momentum is imparted by the particle when it strikes the bucket and also during the subsequent motion until the particle loses contact with the bucket. Torque imparted about X axis due to impact by a single particle having mass m_p.

$$\vec{M}_{initial} = \vec{op}_b \times \vec{F}_i \tag{2.25}$$

where $\vec{op}_b = R\hat{k} + r\hat{r} = (R\cos\theta + r)\hat{r} - R\sin\theta\hat{\theta}$

Torque imparted by the particle about the X axis during the motion on bucket

$$\vec{M}_{\Delta t} = m_p(\vec{o}p_b \times \vec{a}_p) = m_p(-R\sin\theta A_\phi \hat{r} - (R\cos\theta + r)A_\phi\hat{\theta} + (A_\theta(R\cos\theta + r) + A_r R\sin\theta)\hat{\phi}) \tag{2.26}$$

The total torque due to motion of particles on the bucket is

$$\mathrm{M}_{\Delta t} = m_p \sum(\vec{o}p_b \times \vec{a}_p) \tag{2.27}$$

So the net torque= $\sum \mathrm{M}_{\Delta t} + \sum \mathrm{M}_{initial}$, where the summation is over all particles present in the bucket.

2.4 Initial positions of particles

Since particles strike one by one and keep on sliding along the bucket till they lose contact from it, the computation for each particle is done separately from different initial conditions. For a particle on the center line of the jet, the initial position where the particle strikes is:

$$X_c = 0$$

$$Y_c = R\sin\chi + z\sin\chi + y\cos\chi$$

$$Z_c = H = R\cos\chi + z\cos\chi - y\sin\chi$$

where, (X_c, Y_c, Z_c) is the point of impact with respect to the fixed frame, and χ=$(\chi_0 + \omega t)$ is the angle shown in figure (2.1) which varies from χ_0 to χ_{max}, and (x_c, y_c, z_c) are the coordinates of the point of impact on the bucket surface in the moving coordinates system (figure 2.1), and H is the height of the jet above the pivot center O.

It is however unlikely that particle will come only along the center line, as the jet has some finite radius l_0. So we assume that the particle may come along a point randomly located on the circular cross-section of the jet. We do this by assigning a random position to the point by the prescription:

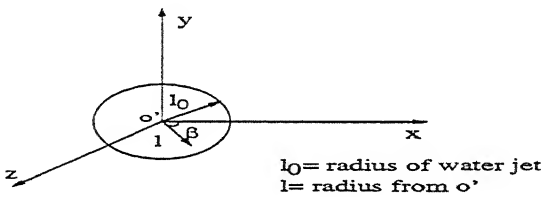

Figure 2.2: Water jet

$$l = l_0\sqrt{ran1}$$

$\beta = 2\pi ran2$

where $ran1$ and $ran2$ are two different uniformly distributed random numbers having values between [0,1] , the random point at any l and β are shown in figure (2.2). This prescription is used to ensure that the points are randomly distributed on the cross section. The initial position of the particles will be perturbed from the center line by :

$\Delta X = l\cos\beta$

$\Delta Z = l\sin\beta$

where ΔX and ΔZ are the variation in the X-direction and the Z-direction, respectively, from the center line. So now the equations for the initial positions are

$$X_p = \Delta X \tag{2.28}$$

$$Y_p = R\sin\chi + z\sin\chi + y\cos\chi \tag{2.29}$$

$$Z_p = H + \Delta Z = R\cos\chi + z\cos\chi - y\sin\chi \tag{2.30}$$

where (x, y, z) is the initial point in the moving frame which has to be determined for a given $\Delta X, \Delta Z, \chi, H$ and R. In these equations, X_p and Z_p are known priori, and Y_p has to be determined in terms of the unknown coordinates y and z which should also satisfy the equation of the bucket surface (chapter 3)

$$\psi(r, \theta, \phi) = 0 \tag{2.31}$$

Thus equation(2.31) has to be converted to a form $Y = f(X, Z)$ and solved to obtain Y_p. This requires a root finding algorithm which is explained below.

The equation of surface $\psi(r, \theta, \phi) = 0$ can be cast as

$$\psi(x, y, z) = 0 \tag{2.32}$$

.

Using equations (2.28), (2.29) and (2.30) we can rewrite the equation $\psi(x, y, z) = 0$ as

$$\psi(X_p, Y_p, Z_p) = 0 \tag{2.33}$$

In equations (2.33) X_p and Z_p are known, and Y_p is the root of the equation. It can be solved using Bisection method. In equations (2.28 to 2.30) we first take a guess value of y, then z is calculated with this guessed value of y using equation (2.30). After getting x, y, z the corresponding r, θ, ϕ are calculated as

$r = \sqrt{x^2 + y^2 + z^2}$

$\theta = \arccos(z/r)$

$\phi = \arctan(y/x)$

The bucket surface is represented as $\psi(r, \theta, \phi) = r - f(\theta, \phi) = 0$ and the data are supplied in the form of a rectangular grid $(M \times N)$ in θ and ϕ at each

grid point of which the radial distance (r) is given. With values of θ, ϕ calculated with the guessed value of y , the radial distance (call r_g) is calculated by linear interpolation of the the θ, ϕ grid. Depending on the magnitude of $r_g - r$, the next guess value of y is taken by the bi-section method. This procedure is repeated till $r_g \approx r$. after getting r, θ, ϕ the x, y, z are obtained by back substitution.

Chapter 3

Representation of Pelton Wheel bucket surface

3.1 Introduction

The primary requirement of our model is to reflect the smallest changes in the surface of the bucket, for which the first step is to represent the bucket surface with very good accuracy.

The surface geometry of a Pelton Wheel bucket is quite complex and obviously can not be represented by a simple analytical function. To overcome this difficulty the bucket surface is represented in the form

$$r = f(\theta, \phi) \tag{3.1}$$

Here data are supplied in the form of a fine rectangular grid $(M \times N)$ in θ and ϕ, and at each grid point the radial distance (r) is given. To calculate the value

of r at any θ and ϕ between the grid points we use bi-linear interpolation. This interpolation is finally done (as explained in the next chapter) in the ODE solver. However the first problem is to create the fine grid representing $r = f(\theta, \phi)$ from a coarse grid of $y = f(x, z)$ data which represents the empirical measurements of the bucket. The fine (r, θ, ϕ) grid is created from the coarse (x, y, z) grid by bi-cubic spline interpolation.

3.2 Bi-cubic spline interpolation

We use the cubic spline interpolation scheme since it provides a superior approximation for functions that may have abrupt local changes. The objective in cubic splines is to derive a third order polynomial for each interval between grid points. In one dimension, the function would be

$$f_j(x) = a_j x^3 + b_j x^2 + c_j x + d_j \tag{3.2}$$

where $j(= 1, 2, 3 \cdots, n)$

To develop cubic splines we have to solve $4n$ equations for the values of a_j, b_j, c_j, d_j for n intervals. These equations are obtained by imposing the conditions that the function yield the tabulated values at the grid points and also the piece-wise functions have continuous first and second derivatives at the grid points.

The second derivatives of the above function can be represented using a first-order Lagrange interpolating polynomial as

$$f_j''(x) = f''(x_{j-1})\frac{x - x_j}{x_{j-1} - x_j} + f''(x_j)\frac{x - x_{j-1}}{x_j - x_{j-1}} \tag{3.3}$$

where $f_j''(x)$ is the value of the second derivative at any point x within the j^{th} $(x_{j-1} \leq x \leq x_j)$ interval. Integrating the equation (3.3) and using function equality conditions, i.e., that $f(x_j)$ must equal the tabulated f_j and $f(x_{j-1})$ must equal f_{j-1}, and invoking the conditions that the first derivatives at grid points must be equal, i.e., $f_j'(x_j) = f_{j+1}'(x_j)$, we get

$$\begin{aligned} & \frac{x_j - x_{j-1}}{6} f''(x_{j-1}) + \frac{x_{j+1} - x_{j-1}}{3} f''(x_j) + \frac{x_{j+1} - x_j}{6} f''(x_{j+1}) \\ = \; & \frac{f(x_{j+1}) - f(x_j)}{x_{j+1} - x_j} - \frac{f(x_j) - f(x_{j-1})}{x_j - x_{j-1}} \end{aligned} \tag{3.4}$$

These $n - 2$ linear equations have n unknowns, all the $f''(x_j)'s$. So setting $f''(x_1)$ and $f''(x_n)$ to zero (which gives the so-called natural spline which has zero second derivatives its boundaries), the above equations can easily be solved by using a tridiagonal matrix algorithm.

In two dimensional interpolation, we seek to create a fine two dimensional rectangular grid $(M \times N)$ of tabulated values from a smaller table of the coarse data. To do this, we perform M one dimensional splines evaluation across the rows of the table, followed by one additional one-dimensional splines down each newly created column. This is called bi-cubic spline interpolation.

3.3 BHEL buckets

Two data sets (say 1 and 2, each representing the surface of a different Pelton Wheel bucket) have been provided by BHEL Bhopal as test cases. We first represent the bucket surface obtained from these data sets by the above mentioned interpolation scheme.

The bucket data are provided in the form of a very coarse rectangular grid in $x - z$ coordinates and $y = f(x, z)$ is provided for (x, z) grid points, along with the coordinates of points on the boundary of the bucket. Referring to figure (3.1), which shows the plan view of the buckets provided, at the points 1a, 2a, etc which lie outside the bucket, the y coordinate value does not have any physical meaning and so are not defined and are kept as blank entries in the input data provided by BHEL. This means that the y coordinate value is not defined at every grid point of the rectangular grid in $x - z$. Implementation of bi-cubic spline interpolation will require complete data on a regular grid. Therefore the first task is to fill these blank entries of input data so that interpolation can be done. The practice used to fill these blank entries is as follows.

First, the y values for the blank entries (grid points 1a,2a,..etc) are extrapolated by any interpolation scheme (polynomial, rational function or cubic spline) along the vertical z direction. If extrapolation is done across a large distance then the extrapolated values given by all schemes are often very unrealistic and make no practical sense; in such cases we abort those values and give some arbitrary value (usually the y value of the neighboring grid point). This will not incur much error

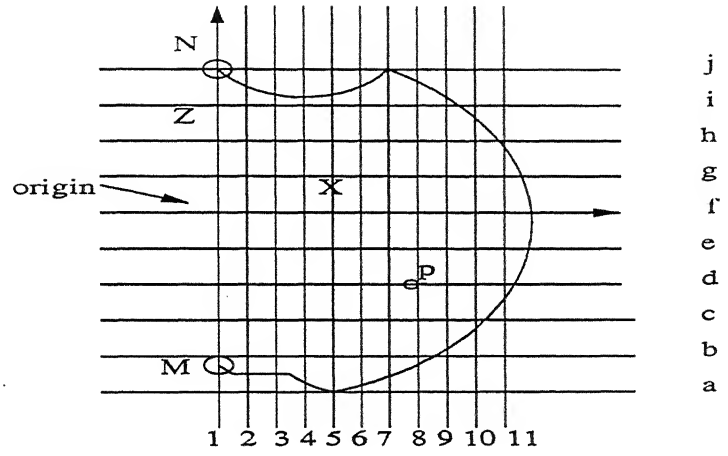

Figure 3.1: $x-z$ projection of the sample case of half of the Pelton Wheel bucket. The data provide y values at each grid point inside the demarcated boundary line.

in the final fine grid bucket representation, as is explained below.

Figure (3.2) shows a bucket which is part of a sine wave 'a', We can see that if the grid point values inside the bucket are represented correctly, the interpolated values within the bucket are interpolated accurately ('c') even if the grid points outside the bucket are abruptly truncated ('b'). Thus the error in the exterior grid points does not affect the interpolation in the interior of the bucket, so the arbitrary extrapolation used does not affect the final fine-grid surface. This feature follows from the local nature of the bi-cubic spline interpolation scheme. The final fine grid surface is used for the particle tracking algorithm.

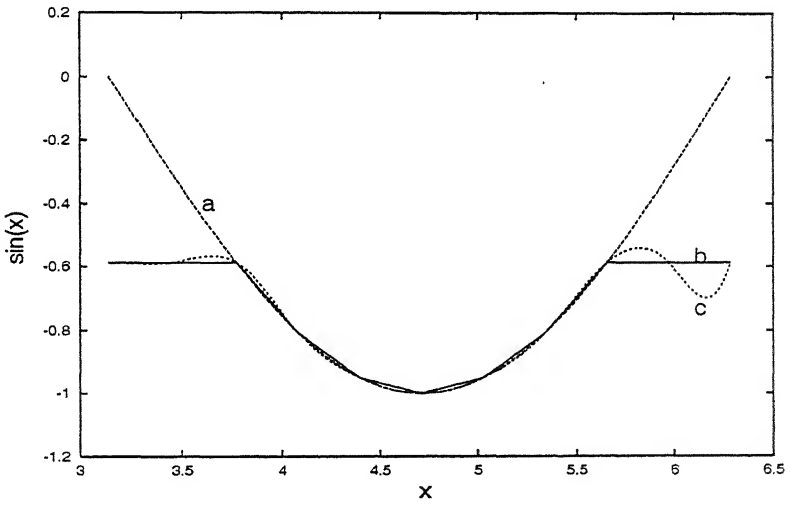

Figure 3.2: property of spline interpolation.
a:the actual sine curve
b:coarse data provided for a sine curve truncated at top
c:interpolated from b using cubic spline interpolation, showing the error introduced at outer edge does not propagate inside.

For the particular cases of the two BHEL data sets, after interpolation of the raw data in vertical direction, the data set 1 was interpolated from a coarse grid of

11×10 to a fine grid of 303×138, while the data set 2 was interpolated from a coarse grid of 10×8 to a fine grid of 278×147. The coarse grids are in x and z, but the fine grids are in θ and ϕ co-ordinates. This change is made for convenience of use in the ODE solver. The maximum limit of θ and ϕ for fine grid is calculated from the boundary as well as the coarse grid.

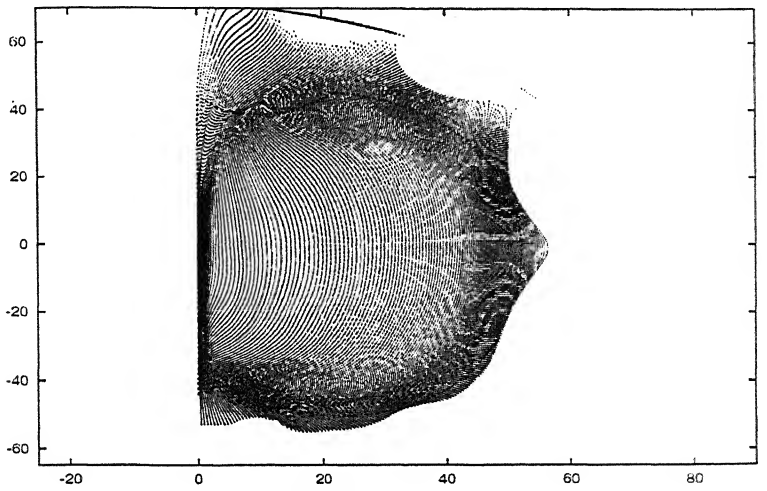

Figure 3.3: $x - z$ projection of the Bucket obtained after bi-cubic spline interpolation for Data Set #1 , provided by BHEL Bhopal as input data.

Fig 3.3 and 3.4 shows the xz projection of the buckets which is obtained after bi-cubic spline interpolation, along with the boundary of the respective buckets. From the two figures (3.3 and 3.4) it is clear that the grid obtained after interpolation contains the actual bucket within it but also has points outside it. Thus it is necessary to identify and mark each (θ, ϕ) grid point as being either within the boundary or outside it. This is done in the following manner.

Since the fine grid is rectangular in θ and ϕ, and at every grid point r, θ and ϕ are known so the x and z coordinate for any grid point are obtained by

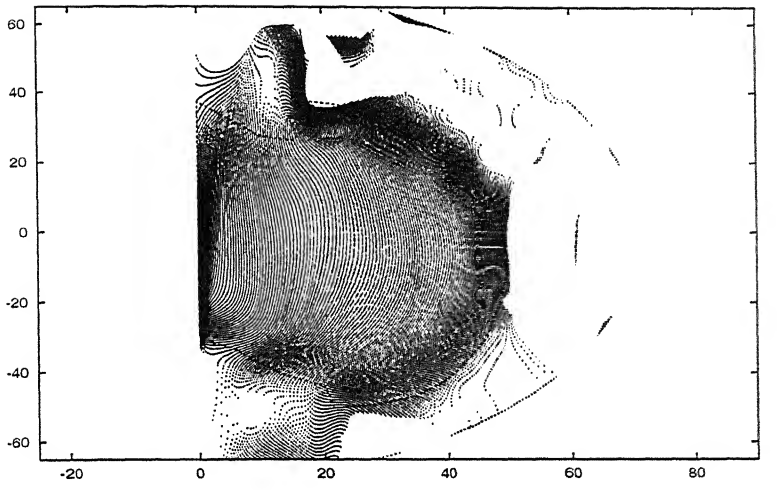

Figure 3.4: $x - z$ projection of the bucket obtained after bi-cubic spline interpolation for Data Set # 2 , provided by BHEL Bhopal.

$$x = r \sin\theta \cos\phi$$

$$y = r \sin\theta \sin\phi$$

$$z = r \cos\theta$$

For each grid point, we can thus find the x and z values from (θ, ϕ) values. For each x, we than find z_{max} and z_{min}, the location of the upper and lower boundaries by linear interpolation of the input boundary data. If the z value of a point in the

bucket surface satisfies $z_{min} \leq z \leq z_{max}$, then it lies within the bucket. For each grid point on the fine grid we first determine whether it is within or outside the bucket, or on the boundary.

We define a cell as a region which is formed by four neighboring grid point, i.e, cell(i, j) is formed by four grid points (i, j), $(i+1, j)$, $(i, j+1)$, $(i+1, j+1)$. If all the four grid points forming a cell lie within the bucket, then the cell has a status 1, which means the cell is within the bucket. The status of cell(i, j) is 0 if all the four grid points forming the cell are outside the boundary, so the cell is completely out of the bucket. The status of cell(i, j) = 2, if one or more, but not all four grid points, are outside the bucket; this is a boundary cell which contains the boundary of the bucket.

In the particle computations, the bucket is assumed to be represented by all cells which have a non-zero status (if the grid is fine this will not incur much error). Figures (3.5 and 3.6) show the buckets represented by only non-zero cells. Thus, with this method the bucket boundary can be closely approximate to the exact one. The grid obtained after this procedure is now used as input to the ODE solver which tracks the particle motion on the bucket surface.

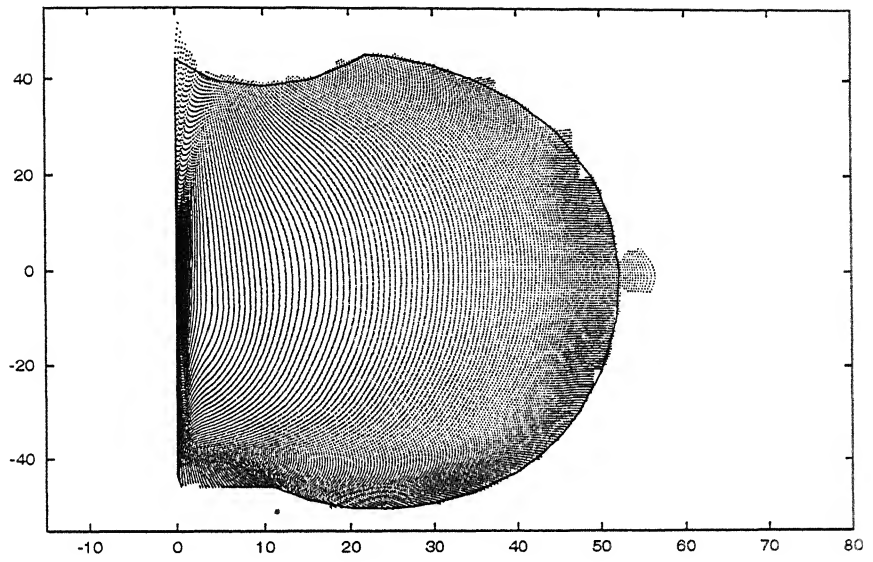

Figure 3.5: Bucket Grid and for Data Set # 1 along with the outer boundary provided by BHEL Bhopal.

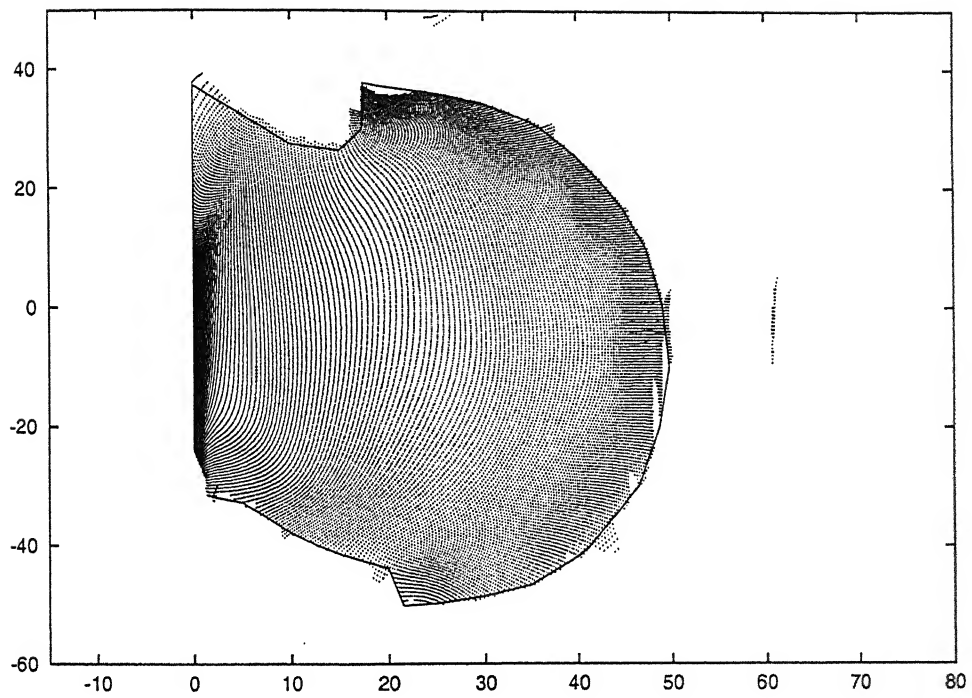

Figure 3.6: Bucket Grid and for Data Set # 2 along with the outer boundary provided by BHEL Bhopal.

Chapter 4

Numerical Methodology

4.1 Introduction

The bucket of a Pelton Wheel has been represented in the form of a fine grid in θ and ϕ. In the governing equations (2.11 and 2.12), which track the motion of the particle on the bucket surface, surface derivatives at every grid point is required. This chapter presents the calculation of the surface derivatives and, if more than one bucket share the jet simultaneously, the method to find which bucket the particle will strike. The algorithm for particle tracking, force & moment calculations and for the integration of many particles information to obtain the overall performance parameters is discussed.

4.2 Calculation of surface derivatives

Our primitive equations (2.11) and (2.12) governing the particle motion on the bucket surface contain the terms $\frac{\partial\psi}{\partial r}$, $\frac{\partial\psi}{\partial\theta}$, $\frac{\partial\psi}{\partial\phi}$, $\frac{\partial^2\psi}{\partial r^2}$, $\frac{\partial^2\psi}{\partial\theta^2}$, $\frac{\partial^2\psi}{\partial\phi^2}$ and $\frac{\partial^2\psi}{\partial\theta\partial\phi}$. As discussed earlier we have reduced the surface presentation of bucket from $\psi(r,\theta,\phi) = 0$ (the equation defining the bucket surface) to a $r - f(\theta,\phi) = 0$ form. So $\frac{\partial\psi}{\partial r} = 1, \frac{\partial^2\psi}{\partial r^2} = 0, \frac{\partial^2\psi}{\partial r\partial\theta} = 0, \frac{\partial\psi}{\partial\theta} = -\frac{\partial f}{\partial\theta}, \frac{\partial\psi}{\partial\phi} = -\frac{\partial f}{\partial\phi}, \frac{\partial^2\psi}{\partial\theta^2} = -\frac{\partial^2 f}{\partial\theta^2}, \frac{\partial^2\psi}{\partial\phi^2} = -\frac{\partial^2 f}{\partial\phi^2}$ and $\frac{\partial^2\psi}{\partial\theta\partial\phi} = -\frac{\partial^2 f}{\partial\theta\partial\phi}$.

The value of r as a function $f(\theta,\phi)$ of θ and ϕ is represented by the fine grid generated by the bi-cubic spline interpolation procedure. We now need to use this data to calculate the derivative of f at any arbitrary (θ,ϕ) point which the particle may be at during its journey on the bucket surface. To ensure continuity of derivatives of the interpolated function across the cell boundaries, the value of first-order, and second-order derivatives with respect to θ and ϕ, is obtained at the grid points using a central difference scheme and the value of the function and these derivatives at any arbitrary point is obtained by linearly interpolating each of these separately. This procedure is elucidated below.

The function value ($f(\theta,\phi) = r$) is available at every grid point on the fine grid. We compute the first and second order derivatives at the grid points using central difference, i.e.

$$\frac{\partial f}{\partial\theta}|_{\theta_i,\phi_j} = f_\theta(\theta_i,\phi_j) = \frac{f(\theta_{i+1},\phi_j) - f(\theta_{i-1},\phi_j)}{2\Delta\theta} \tag{4.1}$$

and similarly,

$$\frac{\partial f}{\partial \phi}|_{\theta_i,\phi_j} = f_\phi(\theta_i, \phi_j) = \frac{f(\theta_i, \phi_{j+1}) - f(\theta_i, \phi_{j-1})}{2\Delta\phi} \tag{4.2}$$

Similarly the second order derivatives at the grid points are computed as follows:

$$\frac{\partial^2 f}{\partial \theta^2}|_{\theta_i,\phi_j} = f_{\theta\theta}(\theta_i, \phi_j) = \frac{f(\theta_{i+1}, \phi_j) - 2f(\theta_i, \phi_j) + f(\theta_{i-1}, \phi_j)}{\Delta\theta^2} \tag{4.3}$$

and similarly,

$$\frac{\partial^2 f}{\partial \phi^2}|_{\theta_i,\phi_j} = f_{\phi\phi}(\theta_i, \phi_j) = \frac{f(\theta_i, \phi_{j+1}) - 2f(\theta_i, \phi_j) + f(\theta_i, \phi_{j-1})}{\Delta\phi^2} \tag{4.4}$$

and the cross-derivatives at the grid-points are computed by

$$\frac{\partial^2 f}{\partial \theta \partial \phi}|_{\theta_i,\phi_j} = f_{\theta\phi}(\theta_i, \phi_j) = \frac{f(\theta_{i+1}, \phi_{j+1}) + f(\theta_{i-1}, \phi_{j-1}) - f(\theta_{i+1}, \phi_{j-1}) - f(\theta_{i-1}, \phi_{j+1})}{4\Delta\theta\Delta\phi} \tag{4.5}$$

At the boundary points a forward difference or a backward difference is used in place of the central difference scheme.

To find the value of the function and its derivatives at the co-ordinates (θ, ϕ), we first find its cell which is bounded by the grid points (θ_i, ϕ_j), (θ_{i+1}, ϕ_j), (θ_i, ϕ_{j+1}) and $(\theta_{i+1}, \phi_{j+1})$, then linear interpolation is used

$$
\begin{aligned}
f(\theta,\phi) = \quad & f(\theta_i,\phi_i)\left(\tfrac{\theta_{i+1}-\theta}{\Delta\theta}\right)\left(\tfrac{\phi_{j+1}-\phi}{\Delta\phi}\right) + \\
& f(\theta_{i+1},\phi_i)\left(\tfrac{\Delta\theta-(\theta_{i+1}-\theta)}{\Delta\theta}\right)\left(\tfrac{\phi_{j+1}-\phi}{\Delta\phi}\right) + \\
& f(\theta_i,\phi_{j+1})\left(\tfrac{\theta_{i+1}-\theta}{\Delta\theta}\right)\left(\tfrac{\Delta\phi-(\phi_{j+1}-\phi)}{\Delta\phi}\right) + \\
& f(\theta_{i+1},\phi_{j+1})\left(\tfrac{\Delta\theta-(\theta_{i+1}-\theta)}{\Delta\theta}\right)\left(\tfrac{\Delta\phi-(\phi_{j+1}-\phi)}{\Delta\phi}\right)
\end{aligned}
\tag{4.6}
$$

where f could be f , f_θ, f_ϕ, $f_{\theta\theta}$, $f_{\phi\phi}$, $f_{\theta\phi}$. This interpolation method is fast and reliable and ensures continuous derivatives across cell boundaries. This last factor is very important, as the particle dynamics can be in error if the derivatives are discontinuous.

4.3 Algorithm for multiple buckets

If the number of buckets in the proposed Pelton wheel design is not already known then the analyses can be carried out for single bucket. However the program is generalized to handle the multi-bucket case, where we know the number of buckets involved.

Figure (4.1) shows the schematic diagram of a jet with buckets as in a practical Pelton Wheel system. The jet is shared by three buckets at a time. In this figure,

The operating range of angles for the given geometry is χ_{min} to χ_{max} which

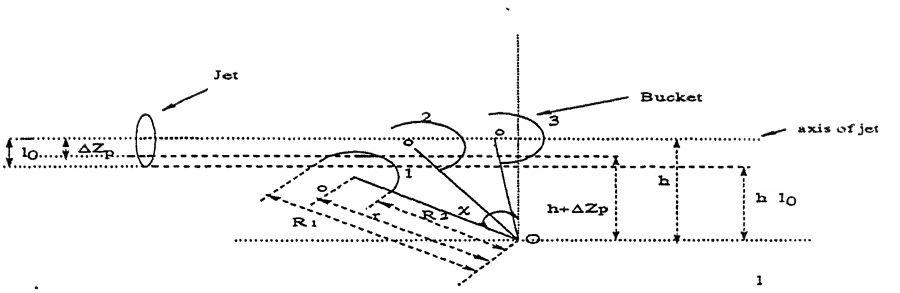

Figure 4.1: Schematic diagram of jet along with the buckets to which it is striking.

are

$$\chi_{min} = -\arccos\left((h - l_0)/R_1\right)$$

and

$$\chi_{max} = \arccos\left((h - l_0)/R_1\right)$$

for a single bucket, where χ_{min} and χ_{max} are the angles at which contact between the jet and the bucket is started and finished respectively.

When a number of buckets are sharing the jet simultaneously, then for pth bucket

$$\chi_{pmin} = \chi_{min} + (p - 1) \times 2\pi/q$$

where p=1,2, or 3 etc., indicate the first, second and third buckets in the 'line of fine' of the jet. Similarly

$$\chi_{pmax} = min\left(\chi_{pmin} + 2\pi/q,\ \chi_{max}\right)$$

where q is total number of buckets in the Pelton Wheel system. The pth bucket starts its motion from χ_{pmin} at $t = 0$ reaching χ_{pmax} at $t = n \times dt$, where n is no of particles $[n = (\chi_{pmax} - \chi_{pmin})\ /(\omega * dt)]$ and dt is the time step. Starting from $t = 0$, particles are assumed to come at regular intervals of dt from random positions in the cross-section of jet.

If a single bucket is moving, then within its range of operating angle, the whole of jet may not strike the bucket and part (depending on the geometry of the bucket) of it may go to waste. As the particles are coming out from random positions in the jet cross-section, therefore it is necessary to know whether the particle coming out at any instant of time strikes the bucket. The contribution of all particles which do not strike the bucket is made zero and their further investigation is not done. Generally the number of buckets in a Pelton Wheel turbine are of the order of 15 -20, therefore at a time the jet is shared by two or more buckets (seldom > 3). Each particle coming from the jet may strike any one of the buckets sharing the jet at that particular instant of time. Since the angular position of buckets are different, the force contribution by the particle will depend on which bucket it strikes. Therefore it is necessary to know which bucket, it strikes. This is checked as follows.

The angle of the arm with the Z axis when pth particle strike at time t_p is χ_p, the coordinates of the particle with respect to center line of the jet are ΔX_p and ΔZ_p. From figures (4.1 and 2.1), the projection of qth bucket on XZ plane at time of impact of pth particle = $(R_1 - R_2)\cos\chi_{pq}\cos\alpha$, where α is the angle of inclination of bucket with its local frame of reference. The Z coordinate of particle with respect to the fixed frame is $h+\Delta Z_p$

If

$$R_2\cos\chi_{p1} < h + \Delta Z_p < R_1\cos\chi_{p1} \tag{4.7}$$

is not satisfied then the particle will not strike the first bucket,

or if

$$R_1 \cos \chi_{p1} \; < h + \Delta Z_p \; < R_1 \cos \chi_{p2} \tag{4.8}$$

is not satisfied along with equation (4.7) then the particle will not strike the second bucket also and will strike to third bucket (note that here $\chi_{p2} = \chi_{p1} + 2\pi/q$ etc. The idea can be extended to more buckets if more share the jet at any time).

However the above criteria considers the vertical (Z coordinate) direction only, and only assures that the particle will *not* strike the bucket if the criteria are *not* satisfied. Fulfilling the above criteria does not assure that particle *will* strike the bucket as it may pass from the side of the bucket. If the above condition is satisfied for the particle striking on *pth* bucket with coordinates X_p and Z_p, solve the equation 2.33 by the scheme mentioned in the second chapter. If X_p and Z_p are such that they are out of the projection of the bucket, the equation will not converge. If the equation does not give a converged solution in a limited number of iterations (say 1000) then the particle is assumed to have missed the bucket and is arbitrarily assigned values of θ and ϕ which must be greater than θ_{max} and ϕ_{max}. As already mention in chapter 3, the bucket is represented by only the cells which have non-zero status. If $\theta_{min} \; < \theta \; < \; \theta_{max}$ *and* $\phi_{min} \; < \phi \; < \phi_{max}$, and the cell to which θ and ϕ belongs have a non-zero status, then the particle is assumed to strike the bucket, otherwise not. If the particle does not strike the bucket then its efficiency of conversion is made zero and its path is not computed.

4.3.1 RK4 solver

The equations (2.11) and (2.12) track the motion of the particle over the bucket surface, and are solved as an initial value problem requiring four initial condition in terms of θ,ϕ, $\dot{\theta}$,$\dot{\phi}$ which are obtained as explained in the second chapter. With these initial conditions the value of θ,ϕ, $\dot{\theta}$,$\dot{\phi}$ at subsequent time steps is calculated by a fourth order Runge-Kutta ODE solver. After each time step we check whether the particle is within bucket or not. The particle can leave the bucket in one of these two ways:

1. If the status of the cell with the new time step values of θ *and* ϕ *is* zero (i.e it is out of bucket), or

2. if the normal acceleration (and hence the force of the particle with respect to bucket) is negative, (i.e., bucket pulls the particle); this means that the particle would lose contact with the bucket.

In applying the second criteria we assume that the particles are non-interacting, But in reality this is not true, because the flow is continuous; so if any single particle's acceleration becomes negative it will try to leave the bucket but will be pushed back by the main stream around it, at the expense of the kinetic energy of the main stream. So two different sets of criteria are applied to check the presence of the particle at each time step

case 1 : The particles are considered as non-interacting and both conditions (1,2) mentioned above are checked. If either occurs, the particle leaves the bucket.

case 2 : Every particle which strikes remains in the bucket till the boundary, thus only the first (1) condition is checked.

4.3.2 Calculation of performance parameters

As already discussed, the ODE solver gives the value of θ,ϕ, $\dot{\theta}$,$\dot{\phi}$ at the next time step. The normal acceleration of the particle is given by

$$a_n = A_r \frac{\partial \psi}{\partial r} + A_\theta \frac{1}{r} \frac{\partial \psi}{\partial \theta} + A_\phi \frac{1}{r \sin\theta} \frac{\partial \psi}{\partial \phi}$$

The velocity and acceleration are computed by calculating the change in the θ,ϕ, $\dot{\theta}$,$\dot{\phi}$ with time, the kinetic energy of each particle is calculated at every time step. The difference between the initial kinetic energy and kinetic energy at exit is used to calculate power (the energy transferred to the bucket) based on kinetic energy approach. It is assumed that there is no energy loss during the motion on the bucket surface, as it is frictionless. In the torque approach the torque (2.25 and 2.26) produced by each particle present in the bucket and the cumulative torque at every time step is calculated after calculating the acceleration of the particle at that time step. The cumulative torque ($T = \Sigma_t \tau$, where τ is the total torque produced at any time step by all particles present in the bucket at that time step) produced for a given bucket angular velocity is used to calculated the energy transmitted.

As already discussed, the particles are represented by the random numbers in the jet cross-section. Therefore, to minimize the effect of randomness in the results, the computations are done for large number of separate simulations. Each

simulation has a separate set of random numbers and hence a separate set of initial positions on the bucket surface where the particles strike. For each simulation, the performance is calculated in the way mentioned above, and finally all the performance parameters are calculated by averaging the results for different simulations. The use of different criteria (for loss of contact) yield slightly different values for the bucket performance parameters, as will be seen in the next chapter.

Chapter 5

Results and Discussion

In this chapter, the performance parameters are calculated for a test case for which the exact analytical solutions are known and thereafter the simulations are done for the two real Pelton Wheel buckets provided by BHEL Bhopal.

5.1 3 D Plane Bucket

The surface over which we study the motion of the particle is a planer surface ABCD as shown in figure (5.1), this surface rotates around the X-axis. The co-ordinate system (xyz) rotates with the plane, and the co-ordinates system (XYZ) is fixed in the lab frame. We also use the spherical co-ordinates (r,θ,ϕ) in the rotating frame with origin o'. The value of r at any arbitrary point (θ,ϕ) is generated using the interpolation scheme. The jet strikes the plane at a height h, coming parallel to Y axis. the jet transmit the power to the plane due to the initial impact,

but the particles then lose contact with the plane. The analytical solution was done for the test case by Gaurav Dar[7]. The comparison of the results by the program with analytical results are shown in table (5.1). it is clear that the test case has good match with exact solution.

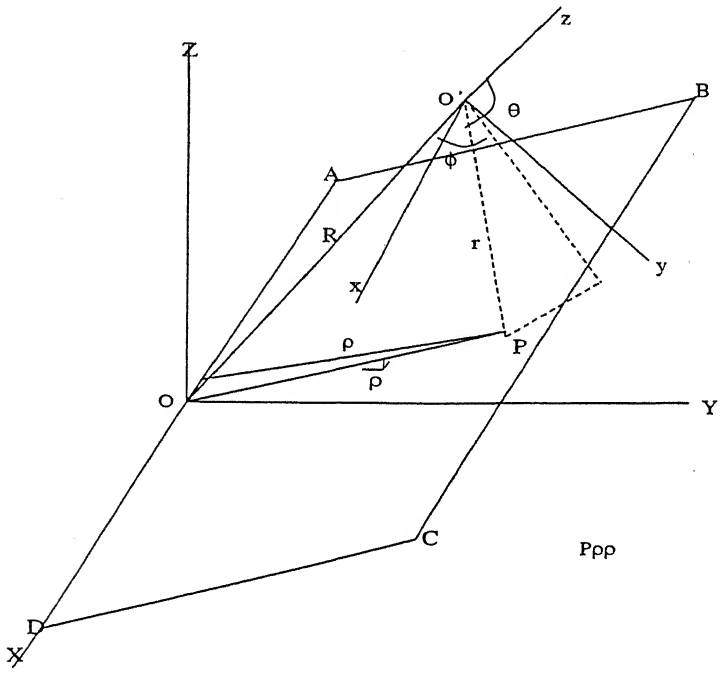

Figure 5.1: Planer bucket in 3D

5.1.1 Analytical solution

The equation for the surface in fig (5.1) with respect to the co-ordinate system (x, y, z) can be written as $y = z + 1$, here the value of R is taken equal to 1, this equation can also be written in the form

$$\psi = r - \frac{1}{\sin\theta \sin\phi - \cos\theta}$$

P is the position of the particle on the bucket surface, its distance from X axis is ρ, which is given by

$$\rho = (y^2 + z^2)^{\frac{1}{2}} = r[\sin^2\theta \sin\phi^2 + \cos^2\theta + \frac{2\cos\theta}{r^2} + \frac{1}{r^2}]^{\frac{1}{2}}$$

The total torque generated by the particle during its motion starting from $t = 0$ to $t = t_f$ is

$$\mathbf{T} = -2\int_0^{t_f} \left(\omega\rho\dot{\rho}\hat{\mathbf{X}} + 2\omega\dot{\rho}X\hat{\rho}\right) dt \tag{5.1}$$

and the total torque exerted along the X-axis during the same time interval is

$$T_X = -2\int_0^{t_f} \omega\rho\dot{\rho}dt \tag{5.2}$$

The power delivered by the particle on the bucket is given by

$$P = -\int T_X\omega dt \tag{5.3}$$

P and ΔKE (change in kinetic energy) should be equal.

Table 5.1: Test case (3 D plane bucket) for the validation of code.

Run	h	$\Delta K_{exact}^{impact}$	P_{exact}^{impact}	ΔK_{num}^{impact}	P_{num}^{impact}
T1	1.0	0.21×10^{-3}	0.12×10^{-3}	0.21×10^{-3}	0.12×10^{-3}
T2	2.0	0.09×10^{-3}	0.08×10^{-3}	0.09×10^{-3}	0.08×10^{-3}

The numerical results are compared with the analytical results for the parameters w, v, h, where ω (angular velocity of bucket) = 0.2, v (vel of jet) =1.0, h is the height of jet above the pivot, P = power due to impact ; ΔK= kinetic energy lost at impact and $P_{in} = mv_j^2 dt/2$ (initial kinetic energy of particle), $\Delta K^{impact} = P_{in} - K_{afterimpact}$. The initial conditions $(\theta_0, \phi_0, \dot{\theta}_0)$ are $\pi/2, \pi/2$ and -0.5 respectively for both test cases, and $\dot{\phi}_0$ is 0. and 0.5 for test case 1 and 2 respectively.

5.2 BHEL buckets

In the following simulations the performance parameters (efficiency, torque and the power output) for the real buckets are found out for 20 separate simulations and then averaged. While calculating for performance parameters both criteria (for loss of contact) as mentioned in the previous chapter are used. Two separate simulations are carried out, one for the single bucket and another for the multi-bucket case where the number of buckets in the system is given as 20. The results obtained for both cases are tabulated below.

5.2.1 Single bucket case

Only one bucket is present in the line of action of jet, the simulation is carried out for the whole span of the bucket in which the jet can strike it.

For Data Set # 1

time step (dt) = 0.0001 sec

χ_{min} =-0.7935, χ_{max} =0.7935 (entire range of striking angle)

R_1=222.12 mm, R_2=126.92 mm (figure 4.1)

angular velocity (ω) =86.5 rad/sec

velocity of jet (v_j)=31 M/sec

radius of jet (l_0)=20.25 mm

inclination angle (α) = 8^0 (rotation of bucket about center of local frame of reference)

total number of particles (n) = 184

For Data Set # 2

time step (dt) = 0.0001 sec

χ_{min} =-0.76178, χ_{max} =0.76178

R_1 = 216.41 mm, R_2 =124.58 mm

inclination angle (α) =4.77^0

total number of particles(n) =178

other input parameters for data set # 2 are same as for data set #1

criteria 1 : Particles are non interacting.

criteria 2 : Particles can leave the bucket only at boundary.

Table (5.2) shows the results for the two buckets. It is clear that first bucket

Table 5.2: The average results for the 20 simulations, for the two loss of contact criteria (1 for non interacting particles, and 2 for particles leaves only at boundary). Here η_1 is the efficiency based on how many particles actually strike the bucket and η_2 is the overall efficiencies based on the total number of particles.

Sr No	Data Set	Criteria	$\eta_1(\%)$	$\eta_2(\%)$
1	1	1	78.52	60.75
2	2	1	59.58	44.18
3	1	2	79.31	62.01
4	2	2	72.77	53.96

is more efficient than the second one from both criteria. Recall that positions of the fluid particles in the jet is random and there is only one bucket, hence not all fluid particles need to actually strike the bucket. Note that in the single bucket case many particles miss the bucket and η_2 is substantially lower than η_1 (which is obtained only for particles which are striking).

5.2.2 Multiple buckets

In a real life Pelton Wheel system, the jet is always shared by two or more buckets at any time (seldom > 3). We have simulated 3 buckets simultaneously sharing the jet (total number of bucket =20). Simulations are done for each bucket individually and the overall performance is calculated by summing up the individual contributions. In chapter 2. it is mentioned that energy transfer by the particle is of two kinds: first, during impact there is loss of kinetic energy and part of the kinetic energy is converted into power (call it impact power), and secondly power transmission occurs as the particles move on the surface of the bucket (i.e power

due to motion). In addition to the overall efficiency, we also compute two other efficiencies η_{impact} and η_{motion}. The first of these tells about the loss (averaged over all particles) of the initial kinetic energy due to the particles' impact with the buckets. Thus

$$\eta_{impact} = \frac{K.E\ after\ impact + power\ transmitted\ to\ bucket\ on\ impact}{Initial\ Kinetic\ Energy}$$

The η_{motion} tells about the amount of kinetic energy lost because of the kinetic energy carried out by the particles finally exiting the bucket.

$$\eta_{motion} = \frac{K.E\ after\ impact - exit\ K.E\ loss}{K.E.\ after\ impact}$$

These two efficiencies give different perspectives on the bucket performance: η_{impact} is used to check whether the operating conditions are optimum or not and η_{motion} basically tells about the optimization of the surface profile. Tables (5.3 to 5.6) shows the results for the two different buckets with different criteria of loss of contact. It is clear from there that η_{motion} is generally lower showing that exit loss are significantly decreasing bucket performance.

To calculate power due to motion we use both the kinetic energy and torque approaches. In the first method, we find power transmitted during motion from the change in kinetic energy of the particles (as motion is assumed to be frictionless). In the second approach, the torque applied by the particles is computed and the power is computed from the torque and the angular speed. The two different methods offer a vital check on the accuracy of the computations, as they should give identical results. It will be shown further that both approaches yield almost same results in our computations, both in terms of numeric values as well as the

qualitative trends. The results for multi-bucket case for both data sets provided by BHEL are tabulated below. In all the cases hereafter, the total efficiencies are based only on the striking particles (as almost all particles strike some bucket).

For both data sets

time step(dt) =0.00003 sec

total number of particles(n)=121

total number of buckets =20, rest of the input parameters are same as in their respective previous cases for single bucket analyses.

Table 5.3: Data Set 1 Criteria 1

Bucket number	1	2	3	Total
$\eta(\%)$	47.84	40.38	0.07	88.29
$\eta^*(\%)$	46.13	38.8	0.07	85.0
$\eta_{impact}(\%)$	53.10	43.41	0.08	96.59
$\eta_{motion}(\%)$	44.31	36.15	0.065	80.53
Impact Power	0.807	1.0397	0.0015	1.848
Impact KE loss	1.0362	1.4645	0.0022	2.503
Power_1 due to motion	8.732	6.7083	0.013	15.453
Power_2due to motion	8.044	6.4069	0.013	14.464
Avg no of particles strike	65.7	55.2	0.1	121

In tables (5.3 to 5.6) η and η^* are the efficiencies calculated based on kinetic energy and torque approaches respectively, subscript 1 is used for power calculated from kinetic energy, and 2 is for torque. All energy and powers are in kW.

The tables (5.3 to 5.6) shows that there is generally a close match between the parameters calculated based on the kinetic energy and the torque approaches. This means the computations are quite accurate (except perhaps in Table 5.4). Also

Table 5.4: Data Set 2, Criteria 1

Bucket number	1	2	3	Total
$\eta(\%)$	38.75	38.15	0.38	77.28
$\eta*(\%)$	34.82	35.66	0.38	70.86
$\eta_{\text{impact}}(\%)$	49.25	43.66	0.66	93.57
$\eta_{\text{motion}}(\%)$	30.71	30.19	0.2	61.1
Impact Power	1.3324	1.8528	0.035	3.22
Impact KE loss	1.769	2.6617	0.051	4.4817
Power_1 due to motion	6.104	5.468	0.038	11.61
Power_2due to motion	5.349	4.99	0.033	10.732
Avg no of particles strike	62.35	57.75	0.9	121

Table 5.5: Data Set 1, Criteria 2

Bucket number	1	2	3	Total
$\eta(\%)$	51.12	41.46	0.07	92.65
$\eta*(\%)$	51.38	41.62	0.07	93.07
$\eta_{\text{impact}}(\%)$	53.10	43.41	0.08	96.59
$\eta_{\text{motion}}(\%)$	49.87	39.2	0.065	89.13
Impact Power	0.807	1.0397	0.0015	1.848
Impact KE loss	1.0362	1.4645	0.0022	2.503
Power_1 due to motion	9.003	6.916	0.013	15.932
Power_2due to motion	9.0528	6.947	0.013	16.013
Avg no of particles strike	65.7	55.2	0.1	121

Table 5.6: Data Set2, Criteria 2

Bucket number	1	2	3	Total
$\eta(\%)$	44.92	41.26	0.59	86.77
$\eta*(\%)$	44.2	41.22	0.59	86.01
$\eta_{\text{impact}}(\%)$	49.25	43.51	0.66	93.42
$\eta_{\text{motion}}(\%)$	41.03	36.65	0.41	78.09
Impact Power	1.332	1.853	0.035	3.22
Impact KE loss	1.769	2.662	0.051	4.482
Power_1 due to motion	7.288	6.061	0.078	13.427
Power_2due to motion	7.148	6.056	0.078	13.283
Avg no of particles strike	62.35	57.75	0.9	121

note that criteria 2 (which seems to be more practical) gives higher efficiencies for the same configuration. Also, the power due to impact is very low and most of the energy conversion takes place during motion of the particle over the bucket surface.

A perfect bucket profile (ideal case) is one in which there is no energy loss at impact (i.e the difference between jet velocity normal to bucket and velocity of bucket in normal direction at the point of impact is zero) then the only energy loss will be the energy carried away by the particle at exit, but real cases are always associated with impact losses and thus lowering the overall efficiency. Therefore efforts are made to reduce the kinetic energy loss at impact by changing the configuration of the system (like height of jet above pivot, pitch circle radius, angular velocity of bucket etc.) with an objective to get the optimum operating conditions for a required power output under given head. Similarly the kinetic energy loss at exit can be reduced by changing the bucket profile. With this program the effect

of changing various parameters as well as the bucket profile on impact kinetic energy loss and the power due to motion can be studied to find out the optimum operating conditions and the bucket surface profile.

The selection of time step (dt) of advancement for ODE solver is also important. As the number of particles depend on time step; the smaller the time step, the larger will be the number of particles being used to simulate the flow. Table (5.7) shows the efficiency variation with time step size for data set # 1 with criteria 2. The results are almost same demonstrating that our results are robust.

Table 5.7: Efficiency for Data Set #1 for different time steps of advancement for the ODE solver

dt /η(%)	1st Bucket	2nd Bucket	3rd Bucket	Total
0.0001	52.71	40.26	-	92.97
0.00003	51.38	41.46	0.07	93.07
0.00001	52.03	40.98	0.08	93.09
0.000005	54.58	38.35	0.18	93.11

Since the jet is modeled as a series of non-interacting plastic particles, each particle has its own independent time history and hence, the efficiency of conversion for each particle is different and depends on the angle of arm with vertical at the time of impact and its position on bucket surface where it makes the impact. Figure (5.2) shows the variation of the efficiency of the particles with respect to the angle of bucket arm with vertical when the particle strikes. Here only one bucket is moving through its full range of operation. It is clear from this figure that the efficiency generally decreases as the rotational angle increases, and the particles which are striking in the last phase of the contact have extremely low

efficiencies thus lowering the average efficiency. Therefore it is not advisable to let the bucket operate in its full range. Clearly the optimum range of average efficiency can be selected from the figure, which will then give the range of angle of operation for each bucket and the number of buckets which will share the jet at any time. Hence the total number of buckets required in the Pelton Wheel can be chosen after fixing the efficiency required. Also larger the number of bucket, the higher will be the average efficiency; but cost will increase, so a compromise between efficiency and the cost can be made.

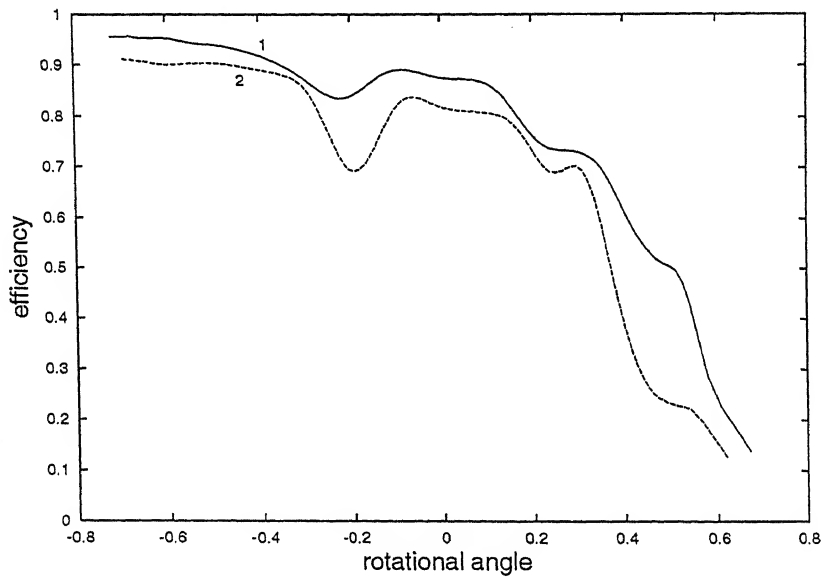

Figure 5.2: Variation of efficiency with rotational angle (jet ratio=8.75)
1. data set #1
2. data set #2

certain

The jet ratio (ratio of pitch circle diameter of Wheel to jet diameter) in the Pelton wheel varies from 5 to 20, the efficiency of the Pelton Wheel turbine is

also depencertaindent on the jet ratio. Figures (5.3 to 5.6) shows the efficiency variation with rotational angle with different jet ratio. It is obvious from the figures that for higher jet ratio (i.e low jet radius), not only is the average efficiency somewhat higher but the curve for efficiency has a lower slope up to a certain rotational angle. This effect is however less prominent beyond a certain jet ratio (in this above 8.75). As the higher jet ratio means lower flow rate and hence less total power output but with higher jet ratio, the maximum number of jets (which can be used with a particular configuration) and hence the power output will increase, therefore the jet ratio should be optimised from efficiency, power output and cost considerations. The present simulations are done (wherever not mentioned) for jet ratio of 8.75.

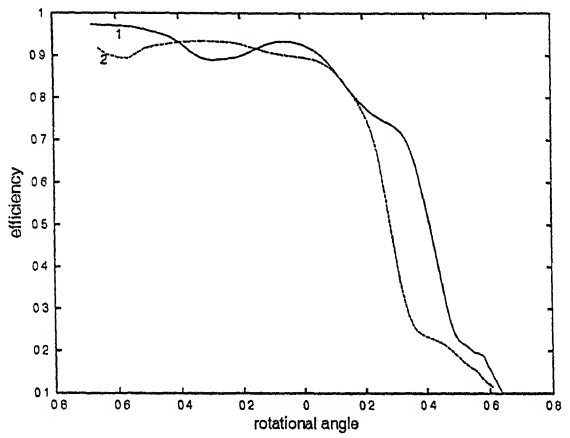

Figure 5.3: Efficiency vs rotational angle (jet ratio =17.7)

If the number of buckets for the proposed design whose performance is to be computed is fixed earlier (from past experience or due to any other constraints) then from the geometry we can know what is the range of operation of a single

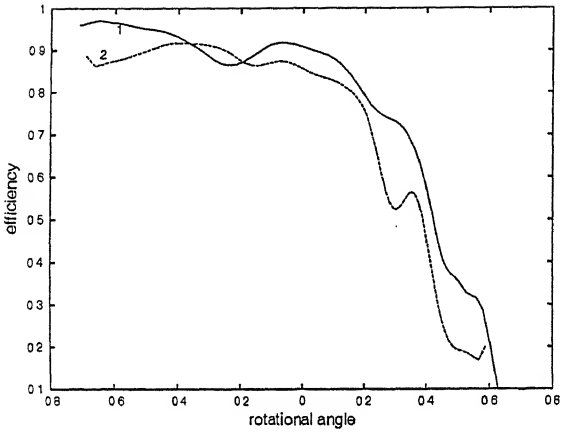

Figure 5.4: Efficiency vs rotational angle (jet ratio=11.82)

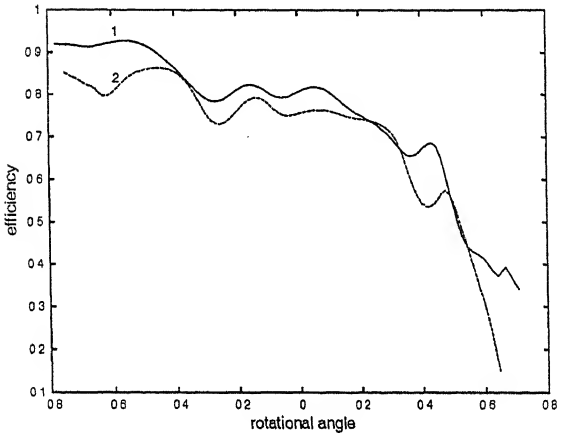

Figure 5.5: Efficiency vs rotational (jet ratio=5.9)

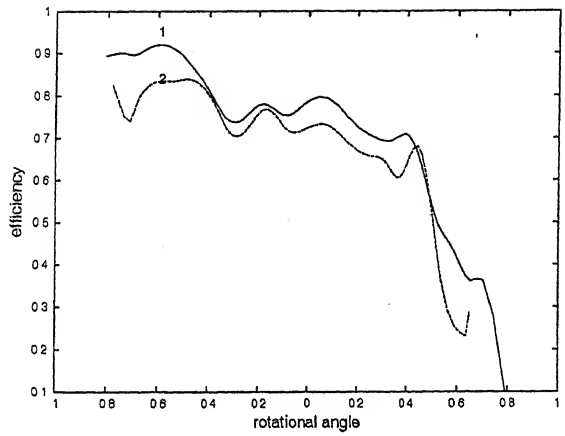

Figure 5.6: Efficiency vs rotational angle (jet ratio=5)

at any time. For a variety of designs it is seen that the number of buckets that share the jet at any time is rarely more than three, this computer model at present computes the case for three buckets simultaneously, but it can be easily extended to as many as required. Figures (5.7) and (5.8) shows the efficiency variation for the two buckets whose results have been discussed, here three buckets are sharing the jet simultaneously, but as clear from the tables that the contribution of the third bucket is very low in comparison with the other two buckets. note that the average efficiency is increased up to a large extent.

When jet is simultaneously striking more than one bucket, each bucket will produce a different torque that depends on the time history of the particle. The total torque and hence the power will be calculated by summing up the individual contribution of each bucket. Figure (5.9 and 5.10) shows the variation of torque with time for each bucket that is sharing the jet for both data set #1 and data set #2 respectively. The total torque variation for both buckets is shown in figure 5.11.

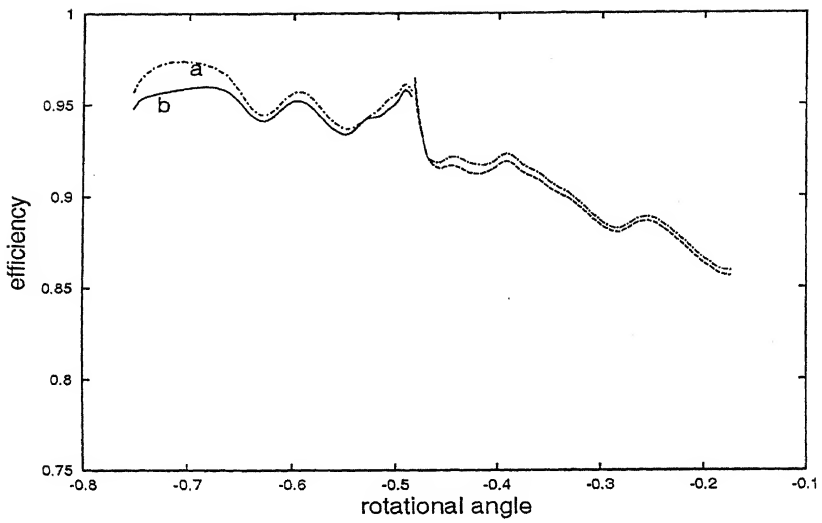

Figure 5.7: Efficiency vs rotational angle for Data Set#1
a. based on torque; b. based on kinetic energy

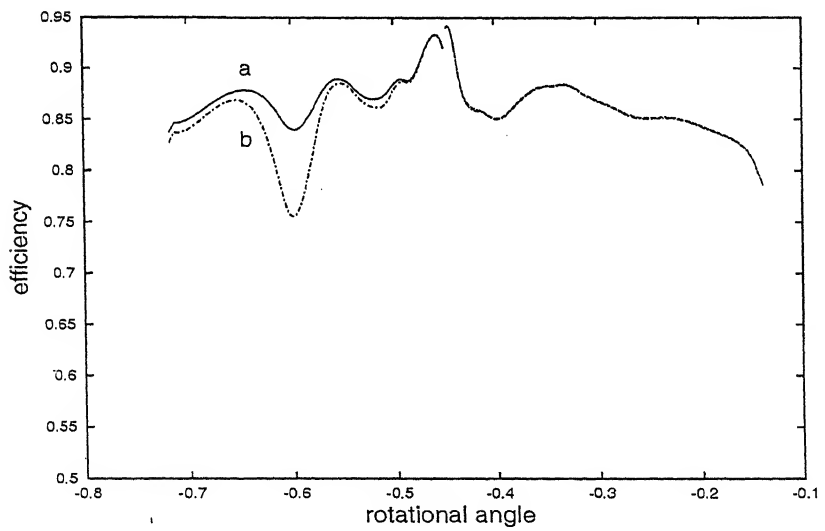

Figure 5.8: Efficiency vs rotational angle for Data Set 2
a. based on torque; b. based on kinetic energy

This figure shows that the bucket is free of fluid within 0.01 seconds. With this knowledge, we can decide how many jets can be used in a multi-jet Pelton Wheel.

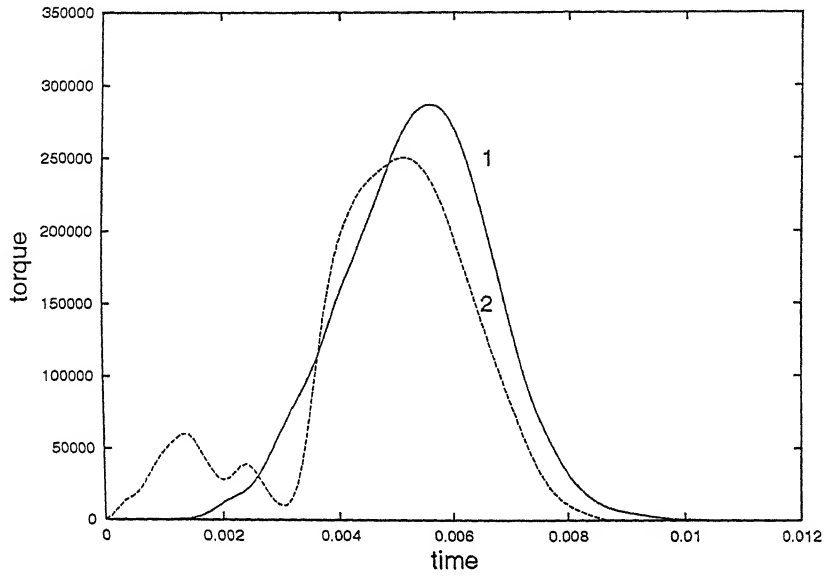

Figure 5.9: Variation of total torque with time for data set #1
1, 2 are the the buckets which are sharing the jet

It has been already discussed that each particle has its own independent time history. Thus the path of each particle can be traced while moving over the bucket surface. Figures (5.12) and (5.13) show the path of few particles with their individual efficiency of conversion (criteria 2) for data set 1 and 2 respectively. Since the efficiency of conversion of each particle is known, by tracking the path of particles over the bucket surface we can locate the regions in the bucket surface which give low efficiencies.

The path of particles over the bucket surface using criteria 1 (non interacting particles) shows (figures 5.14 and 5.15) that some particles leave the bucket in the

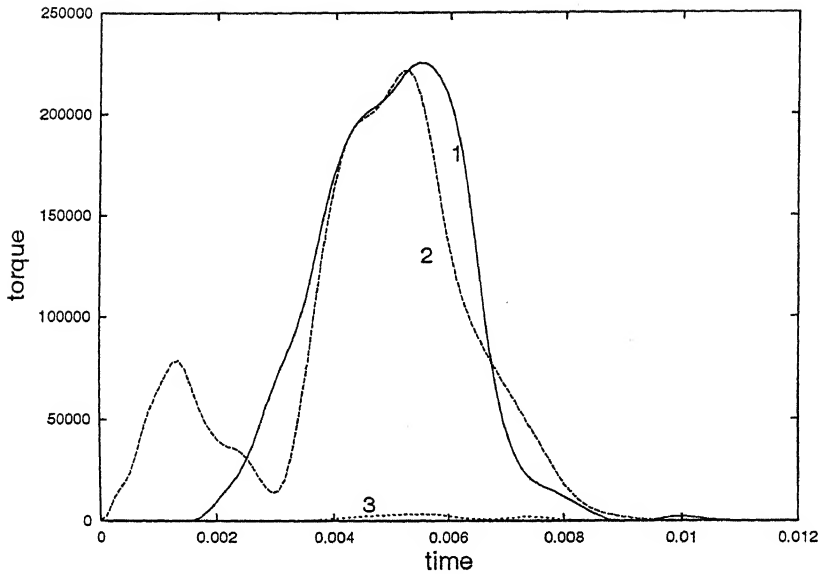

Figure 5.10: Torque vs time for data set #2
1, 2, 3 are the three buckets to which jet is striking simultaneously.

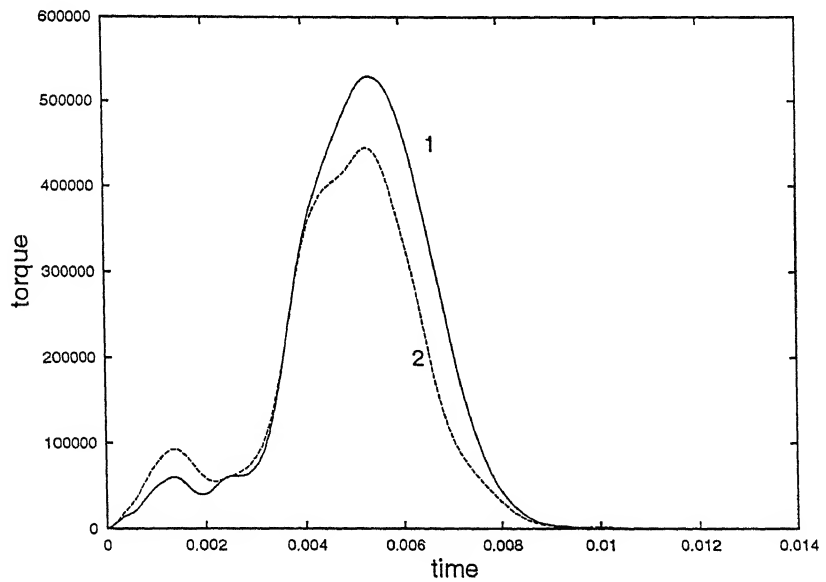

Figure 5.11: Total torque vs time

1. Data Set # 1
2. Data Set # 2

middle. This indicates local irregularities in the surface of bucket at those places where the particle has left the bucket, by modifying these areas the bucket surface can be optimized. For a perfect bucket surface the performance of the bucket with both criteria should be equal, so closer the performances of the bucket with two different criteria mentioned above, nearer the bucket surface will be to the optimum one.

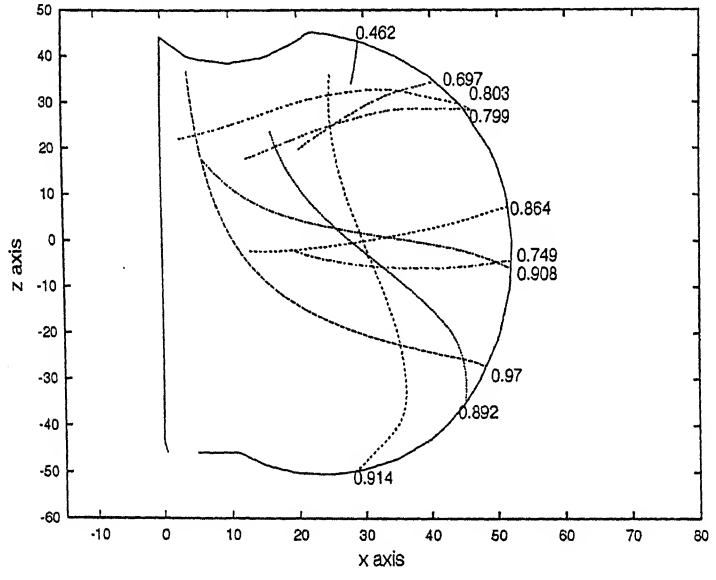

Figure 5.12: Path of few particles with their efficiency while moving over the bucket surface obtained for data set #1, criteria 2 (jet ratio=5)

The results for the above mentioned buckets have been found to have close match with the experimental results of BHEL Bhopal. The program was tested by varying the input parameters, the trend as well as the prediction of the performance parameters were found to be on the right track.

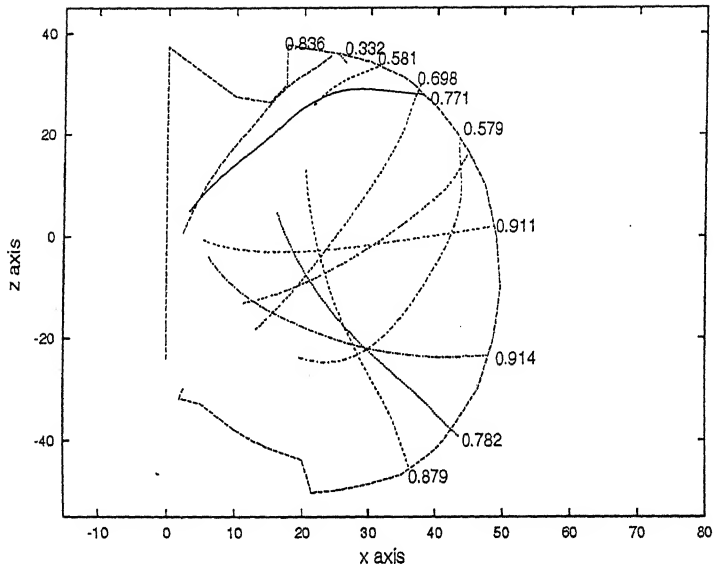

Figure 5.13: Path of few particles with their efficiency while moving over the bucket surface obtained for data set #2, criteria 1 (jet ratio=5)

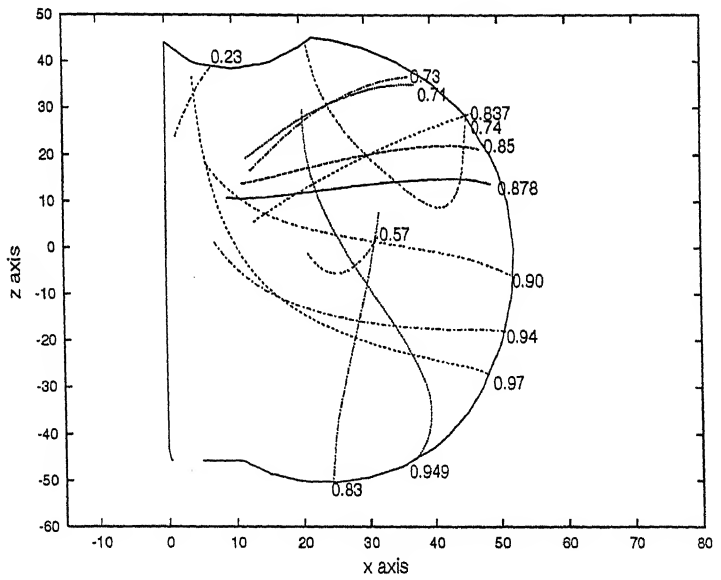

Figure 5.14: Path of few particles with their efficiency while moving over the bucket surface obtained for data set #1, criteria 1 (jet ratio=5)

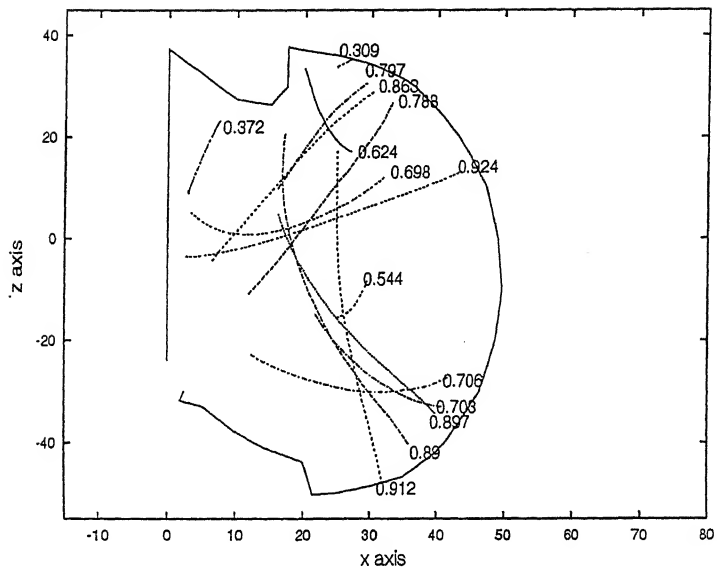

Figure 5.15: Path of few particles with their efficiency while moving over the bucket surface obtained for data set #2, criteria 1 (jet ratio=5)

5.3 Conclusion and future work

In this thesis, the program which started by Ajay Kumar and followed by Gaurav Dar, is now fully developed. One test case (also tested by Gaurav Dar during development stage of the program) is simulated with the completely developed program, and finally the performance parameters for two Pelton Wheel buckets are computed and compared. The complete program is developed to handle a variety of cases and to simulate the effect of any of the input parameters, the present program is tested against large set of experimental results and found to be quite sensitive to the surface changes which was the prime requirement. Thus this program is extremely useful for industrial application. It can act as a tool to a designer by which he can calculate the performance parameters of a Pelton Wheel

numerically These parameters includes

1. The overall efficiency of the bucket.
2. The kinetic energy loss associated with impact (η_{impact}).
3. The kinetic energy exit loss (η_{motion}).
4. The efficiency vs arm angle (χ) curve, which tells at what striking angles the performance is good.
5. The particle paths can be used to correlate lower efficiency obtained (for certain angles) with portions of the bucket surface. This will help in locating the less optimum portions of the bucket surface.
6. Total power output of the complete Pelton Wheel.
7. Torque variation of individual buckets and the total torque variation with time.
8. Number of jets which can be used with given configuration and bucket surface profile.

The program gives the liberty to the designer to think of many different designs for a particular requirement, since different designs can be tested and compared with the help of the program and the most efficient can be found. The most efficient design can be further optimized by analyses of particle's individual efficiency and its path over the bucket surface. Also the most optimum operating conditions for

the required output can be found out by changing the operating conditions and studying its effect on the amount of kinetic energy loss at impact.

In the future the present work can be extended for non-friction surface. The further work can include the vibration of rotor and its effect on performance of the Wheel. Attention can also be paid upon the water jet which is assumed to be running in straight line while in reality it has some curvature. Here the fluid coming out from the jet is considered as a cylindrical stream, while in practical cases due to the presence of a spear rod the fluid flow is like flow between two concentric cylinders where the inner cylinder radius is quite small.

Bibliography

1. Ferdinand P.Beer and E.Russell Johnson, Jr.,Vector Mechanics for engineers, McGraw-Hill Book Company.

2. K.Murlidhar and T.Sundarajan, Numerical Fluid Flow and Heat transfer, Narosa Publishing House.

3. J.Vesely and F.Pochyly, Particle path on a Pelton turbine bucket, Hydro Power -III, Oct 1998.

4. A.K.Jain, Fluid Mechanics, Khanna publishers, New Delhi.

5. Jagdish Lal, Hydraulic Machines, Metropolitan book co. pvt. Ltd., New Delhi

6. Ajay Kumar, "A Particle Dynamics Model For Evaluation Of Efficiency Of A Pelton Wheel Bucket", M.Tech Thesis, I.I.T Kanpur, Jan, 1999

7. Gaurav Dar, "A 3 -D test case for the Pelton Wheel particle tracking algorithm ", A Project Report to BHEL Bhopal by I.I.T Kanpur, April 2001